

3DXTALKER: UNIFYING IDENTITY, LIP SYNC, EMOTION, AND SPATIAL DYNAMICS IN EXPRESSIVE 3D TALKING AVATARS

Zhongju Wang*

University of New South Wales
zywang9691@gmail.com

Zhenhong Sun*

Australian National University
zhenhongsun1992@outlook.com

Beier Wang

University of New South Wales
beier.wang@unsw.edu.au

Yifu Wang

Vertex Lab
usasuper@126.com

Daoyi Dong

University of Technology Sydney
daoyidong@gmail.com

Huadong Mo[†]

University of New South Wales
huadong.mo@unsw.edu.au

Hongdong Li

Australian National University
hongdong.li@anu.edu.au

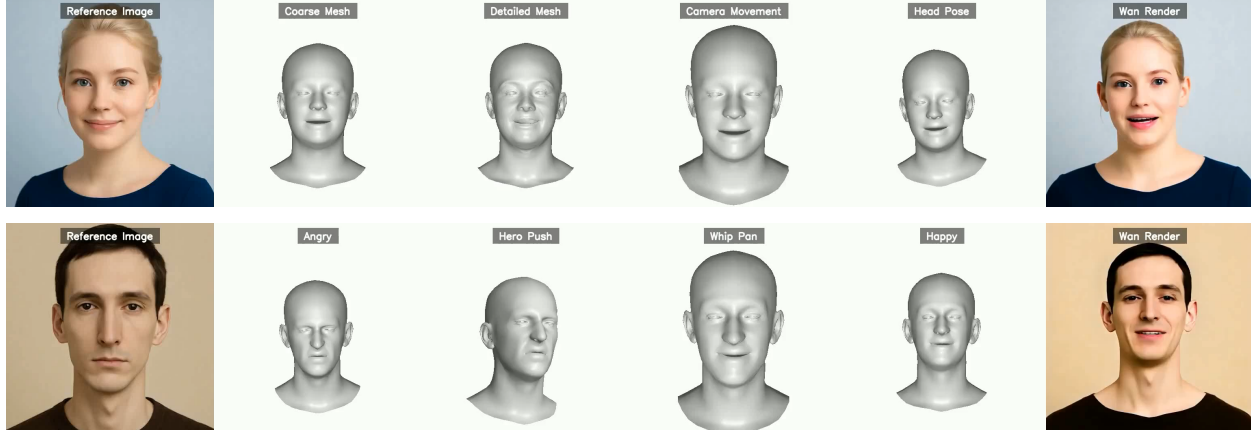


Figure 1: Overview of our expressive 3D talking avatar generation. Given a single reference image and a driving speech audio, 3DXTalker produces identity-consistent 3D talking avatars with accurate lip synchronization, expressive emotions, and natural head-pose dynamics. Homepage is available at <https://engineeringai-lab.github.io/3DXTalker.github.io/>.

ABSTRACT

Audio-driven 3D talking avatar generation is increasingly important in virtual communication, digital humans, and interactive media, where avatars must preserve identity, synchronize lip motion with speech, express emotion, and exhibit lifelike spatial dynamics, collectively defining a broader objective of expressivity. However, achieving this remains challenging due to insufficient training data with limited subject identities, narrow audio representations, and restricted explicit controllability. In this paper, we propose 3DXTalker, an expressive 3D talking avatar through data-curated identity modeling, audio-rich representations, and spatial dynamics controllability. 3DXTalker enables scalable identity modeling via 2D-to-3D data curation pipeline and disentangled representations, alleviating data scarcity and improving identity generalization. Then, we introduce frame-wise amplitude and emotional cues beyond standard speech embeddings, ensuring superior lip synchronization and nuanced expression modulation. These cues are unified by a flow-matching-based transformer for

*Equal Contribution

[†]Corresponding Author

coherent facial dynamics. Moreover, 3DXTalker also enables natural head-pose motion generation while supporting stylized control via prompt-based conditioning. Extensive experiments show that 3DXTalker integrates lip synchronization, emotional expression, and head-pose dynamics within a unified framework, achieves superior performance in 3D talking avatar generation.

1 Introduction

Audio-driven 3D talking avatar generations [1, 2, 3, 4] have been extensively applied across various domains. By mapping audio signals (speech or singing) to realistic 3D facial movements, these systems provide a natural way to animate avatars without requiring complex 3D capture hardware. Early approaches [5, 6, 7] largely focused on producing basic lip movements or coarse facial animation, which underperformed against the emerging demand for personalized, natural move and communicative avatars. As applications evolve, the field has shifted toward a more comprehensive goal: achieving *expressivity*, where avatars could preserve identity, synchronize lips with speech, express emotions, and exhibit lifelike spatial, shown as Figure ??.

Despite notable progress [8, 9, 10, 11], achieving comprehensive expressivity remains an ongoing challenge, primarily due to three key factors: insufficient training data with limited identity diversities, narrow audio representations, and restricted explicit controllability. Existing 3D audio-mesh datasets [12, 13, 14] rely on costly, complex real-world capture, while many modeling paradigms [15, 5, 9] couple identity with motion patterns, resulting in limited identity diversity, emotion, and spatial motions, which hinders the models’ scalability and generalization. Meanwhile, commonly used audio representations mainly capture linguistic content [16, 17] (e.g., Wav2Vec [18]), while under-representing prosodic cues, e.g., amplitude variation and emotional tone, are critical for accurate lip movements and expressive facial emotions. Moreover, explicit controllability is often limited, and most talking heads are generated in a largely static or front-facing configuration and ignore camera motion during rendering [19, 20, 21], constraining the ability of user-defined spatial dynamics. These limitations collectively hinder a model’s ability to capture the full spectrum of speech-driven expressivity for identity, lip sync, emotion, and spatial dynamics.

Generating identity-diverse 3D talking heads is challenging because high-quality 3D data is scarce, while 2D videos provide abundant identities, emotional styles, and natural motion patterns at scale. Facial representation models, such as DECA [22] and EMOCA [23], could lift video frames into FLAME shape-expression-pose parameters [24], effectively bridging 2D video and controllable 3D facial modeling. Building on this paradigm, we construct a 2D-to-3D data-curated identity modeling pipeline. We collect three lab-controlled datasets (GRID [25], RAVDESS [26], MEAD [27]) and three in-the-wild datasets (VoxCeleb2 [28], HDTF [29], CelebV-HQ [30]). A unified filtering pipeline is then applied for duration, language, audio-visual sync, and resolution to ensure data quality and diversity. We build structured frame-referred FLAME parameters using EMOCA, leveraging its disentangled latent space to separate stable identity attributes from temporally varying lip, expression, and pose motions. This yields a dataset with rich identity coverage, lip and emotional variations, and lifelike spatial dynamics, without relying on 3D capture.

Utilizing the above pipeline, we introduce **3DXTalker**, an integrated flow-matching framework that operates in the disentangled FLAME parameter space to generate expressive 3D talking-head motion sequences conditioned on a reference image and driving audio. Beyond conventional audio embeddings for lip sync, we incorporate frame-wise amplitude features for coherent mouth aperture and frame-wise emotion features for nuanced expression modulation. This forms **audio-rich representations** that more faithfully reflect the dynamics of speech. The image-derived identity latent and audio-derived motion cues are jointly modeled via a multi-branch transformer, which produces identity-consistent, emotionally aligned talking-head motion. To further enhance **dynamic controllability**, we enable scalable adjustment of global expression intensity, and optionally incorporate LLM-driven head-pose modulation. Collectively, these designs make 3DXTalker simultaneously achieve identity consistency, lip-sync accuracy, emotional expressions, and diverse spatial dynamics in a single paradigm.

The main contributions are summarized as follows:

- We construct a scalable 2D-to-3D data-curated identity modeling with disentangled representation, mitigating both the limited dataset and identity diversity problems.
- We introduce frame-wise amplitude and emotion cues beyond standard speech embeddings, to further improve lip synchronization and emotional expressions.
- We integrate these advances into **3DXTalker**, a comprehensive system that jointly achieves holistic expressivity in 3D talking avatars, while supporting controllable head-pose generation and emotion diversity.

2 Related Work

3D Identity Modeling and Avatars. Audio-driven 3D avatar synthesis relies on parametric or non-parametric mesh representations. Parametric models, such as 3D Morphable Model [31], Basel Face Model [32], and FLAME [24], use low-dimensional shape, expression, and pose parameters to represent facial geometry, enabling 2D-to-3D learning methods [22, 23, 33, 34]. In contrast, non-parametric approaches model facial surfaces at the vertex or point-cloud

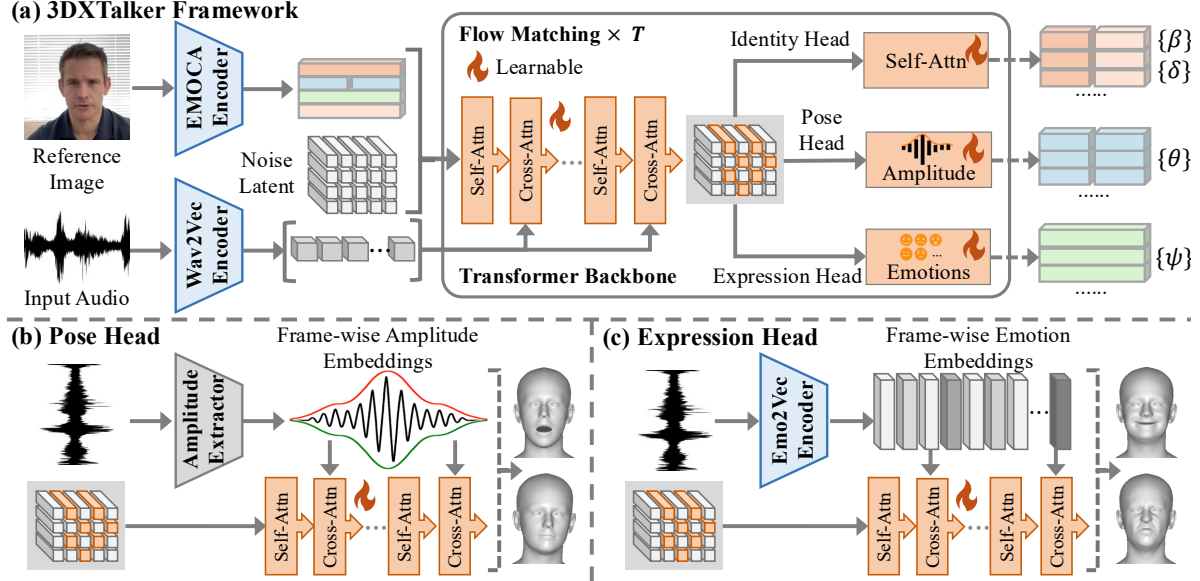


Figure 2: Overview of 3DXTalker framework. (a) A multi-branch flow-matching transformer fuses identity and audio cues to model disentangled FLAME parameter space. (b) Frame-wise audio amplitude contributes to coherent mouth aperture and head dynamics. (c) Frame-wise emotion embeddings help modulate emotional expressions.

level for greater expressiveness. Building on these representations, recent works [6, 7, 35, 36, 37, 38] animate 3D heads from audio, evolving from deterministic regression mappings to generative models.

Regression Models with Audio. Early methods adopt regression frameworks that deterministically map audio to 3D facial motion. Most extract features from large-scale self-supervised speech models, such as Wav2vec 2.0 [18], HuBERT [16], and WavLM [17], and regress either raw vertex displacements [5, 39, 40, 41] or parametric model latents [10, 42, 43, 15, 44, 9, 8, 45]. FaceFormer [5] predicts vertex trajectories using a transformer decoder, while UniTalker [15] and CodeTalker [44] compress facial motion into low-dimensional latents for efficient prediction.

Generative Models with Audio. To improve the diversity and realism of audio-driven 3D facial animation, recent work has increasingly adopted generative formulations that model the conditional distribution from speech audio to facial motion. VQ-VAE-based methods (e.g., Learn2Listen [42], DEEPTalk [10]) discretize facial motion into latent code sequences and sample them conditioned on audio, while diffusion-based approaches (e.g., FaceDiffuser [46], DiffPoseTalk [11], DiffusionTalker [47], FaceTalk [20]) generate motion by progressively denoising from Gaussian noise, yielding higher variation and realism. Despite these advances in lip synchronization, existing methods typically enhance expressivity along other dimensions. For instance, EMOTE [8] focuses on modeling emotional facial expressions, while DiffPoseTalk explores audio-driven head-pose dynamics as a separate component. We therefore propose an integrated framework that unifies these three components for comprehensively enhancing expressive 3D talking avatar generation.

3 Method

In the task of 3D audio-driven talking avatar generation, the objective is to synthesize a sequence of 3D avatar states $\{\mathbf{M}_i\}_{i=1}^N$ (N total frames) that align with a given audio waveform \mathbf{A} , ensuring precise synchronization between facial movements and speech. Beyond lip-sync, modern avatar systems are increasingly expected to achieve **expressivity**, which encompasses consistent identity preservation, emotion-aware facial expressions, and realistic spatial dynamics that enhance communicative impact. Meanwhile, there remains room to further enhance expressivity by expanding dataset and identity diversity for better generalization, enriching audio representations to capture richer prosodic patterns and emotional cues, and strengthening explicit controllability for more interpretable and precise manipulation of avatar dynamics. To meet the diverse requirements of expressivity, we propose an integrated framework, 3DXtalker, that enhances avatar generation across four dimensions: identity consistency, lip synchronization, emotion expressions, and spatial dynamics controllability, as detailed in the following subsections.

3.1 Data-curated Identity Modeling

EMOCA Modeling Preliminary. To leverage the abundant identities, emotional styles, and dynamic motion patterns in 2D videos, we adopt the EMOCA parametric autoencoder [23], which projects video frames into a controllable 3D facial parameter space. The model encodes 2D images into FLAME parameters [24], including shape $\beta \in \mathbb{R}^{100}$, pose $\theta \in \mathbb{R}^6$, expression $\psi \in \mathbb{R}^{50}$ and an additional detail parameter $\delta \in \mathbb{R}^{128}$. Then, they can be decoded into a coarse mesh $\mathbf{M}_{coa} \in \mathbb{R}^{5023 \times 3}$ deformed from a FLAME template $\bar{\mathbf{V}}$ with β , ψ and θ , which is refined by detail decoder \mathcal{D}_{det} to form a detailed mesh $\mathbf{M}_{det} \in \mathbb{R}^{59315 \times 3}$ through facial displacement map, formally defined as:

$$\begin{aligned} \mathbf{V}_{int} &= \bar{\mathbf{V}} + \mathbf{B}_S(\beta) + \mathbf{B}_E(\psi), \\ \mathbf{M}_{coa} &= \text{LBS}(\mathbf{V}_{int}, \mathbf{J}_P(\bar{\mathbf{V}}), \mathcal{W}, \theta), \\ \mathbf{M}_{det} &= \mathbf{F}_{det}(\mathbf{M}_{coa}, (\bar{\mathbf{U}} + \mathcal{D}_{det}(\theta, \psi, \delta))), \end{aligned} \quad (1)$$

where \mathbf{V}_{int} is an intermediate mesh, \mathbf{B}_S and \mathbf{B}_E are shaping and expressing functions, LBS denotes the linear blend skinning algorithm with joint regressors \mathbf{J}_P and skinning weights \mathcal{W} , $\bar{\mathbf{U}}$ denotes template UV map, and \mathbf{F}_{det} applies the predicted displacement map to the coarse mesh \mathbf{M}_{coa} . Notably, the pose parameter θ can be decomposed into *head pose* and *jaw pose*, allowing head motion to be modeled and controlled through simple linear variations. This parameterization provides a disentangled and controllable 3D facial representation, which serves as the foundation for our subsequent data-curated identity modeling pipeline. Further details of this process are provided in **Appendix A**.

Dataset Curation Pipeline. We construct a diverse data corpus by combining three lab-controlled datasets (GRID [25], RAVDESS [26], MEAD [27]) with three in-the-wild datasets (VoxCeleb2 [28], HDTF [29], CelebV-HQ [30]). The lab-controlled datasets provide high-quality recordings with articulated facial movements and emotional expressions, while the in-the-wild datasets introduce a broad range of identities, speaking styles, and natural spatial dynamics. To ensure data reliability across sources, we apply a unified filtering pipeline comprising: (1) duration thresholding to stitch video clips exceeding 10 seconds, (2) signal-to-noise ratio filtering to suppress noisy or corrupted speech, (3) language filtering to maintain linguistic consistency, (4) audio–visual synchronization verification to eliminate misaligned segments, and (5) spatial resolution normalization to 512×512 . (Further details provided in **Appendix B.1**.) Each video frame is then lifted into the FLAME parameter space via EMOCA [23], yielding a structured representation that consists of identity shape β and detail δ , as well as frame-varying expression ψ and head pose θ . To construct a temporally consistent representation that disentangles identity from motion, we take the first frame as the reference and express all parameters in a differential form:

$$\mathbf{X}_\Delta = \{(\beta_i - \beta_0, \delta_i - \delta_0, \psi_i - \psi_0, \theta_i - \theta_0)\}_{i=1}^N. \quad (2)$$

This representation enables identity stability while lip movements, expressions, and head dynamics evolve over time. The resulting parametric sequence thus forms a consistent, controllable, and compact 3D facial motion trajectory, which serves as the basis for the subsequent generative modeling in our framework.

3.2 Unified Audio-rich Framework

Overview. The data-curated identity modeling pipeline obtains disentangled identity and motion representations from 2D videos using EMOCA. This allows a single reference image to serve as a reliable identity anchor during generation, in contrast to prior 3D audio-driven methods that relied on a fixed identity template. Additionally, the audio side remains a limiting factor. Speech signals inherently contain multiple layers of information: (1) linguistic content (word, phoneme), (2) articulatory dynamics reflected in amplitude and rhythm that drive jaw motion and mouth aperture, and (3) emotional prosody conveyed through intonation, energy contours, and vocal timbre. Common audio embeddings focus on linguistic content [18, 16, 17], but overlook prosodic cues, leading to correct word synchronization but weak mouth aperture and flat emotion expressions.

To address this gap, we introduce **3DXTalker**, an integrated flow-matching framework that operates in the disentangled parameter space to generate expressive 3D talking-head sequences conditioned on a reference image \mathbf{I}_0 and driving audio \mathbf{A} . Beyond conventional audio embeddings, we incorporate frame-wise amplitude features for coherent mouth aperture and frame-wise emotion features for nuanced expression modulation, forming **audio-rich representations** that more precisely reflect the dynamics of speech. The identity latent derived from the reference image and the audio cues is then jointly modeled through a multi-branch flow-matching transformer, enabling identity consistency, lip synchronization, and emotional alignment in talking-head motion, as depicted in Figure 2. We next outline the inference process of this framework.

Transformer Backbone. Given an input image \mathbf{I}_0 , we first extract the reference parametric representation $\mathbf{X}_{ref} = (\beta_0, \theta_0, \psi_0, \delta_0) \in \mathbb{R}^{1 \times 284}$, which is then combined with t step-dependent noise $\varepsilon_t \in \mathbb{R}^{N \times 284}$ (initial random noise ε_0) to form the model’s input state $\tilde{\mathbf{X}}_t$ after the MLP layers. The input audio \mathbf{A} is processed into linguistic embeddings $\mathbf{A}_{feat} \in \mathbb{R}^{N \times d}$ (d represents dimension) using WavLM [17]. In the Transformer backbone \mathcal{D}_{flow} , $\tilde{\mathbf{X}}_t$ serves as queries, while the audio embeddings \mathbf{A}_{feat} act as keys and values. Through self-attention and cross-attention, the

model produces the intermediate latent representation \mathbf{H}_t . The overall process can be summarized as follows:

$$\begin{aligned}\tilde{\mathbf{X}}_t &= \text{MLP}(\varepsilon_t) + \text{MLP}(\mathbf{X}_{ref}), \\ \mathbf{H}_t &= \mathcal{D}_{flow}(\tilde{\mathbf{X}}_t, \mathbf{A}_{feat}, t).\end{aligned}\tag{3}$$

\mathbf{H}_t serves as the fused latent representation that integrates the reference identity and the linguistic content from audio and is subsequently passed through three parallel branches to disentangle and predict different FLAME parameters.

Identity Head. This branch is responsible for predicting the shape $\{\beta\}$ and detail $\{\delta\}$ parameters that define the identity of the generated talking head. With the global latent representation \mathbf{H}_t extracted, the identity head employs lightweight self-attention layers \mathcal{D}_{id} to further form identity-related features and subsequently passes them through an MLP layer to produce the velocity field of shape and detail ($\hat{\mathbf{v}}_t^\beta \in \mathbb{R}^{N \times 100}$ and $\hat{\mathbf{v}}_t^\delta \in \mathbb{R}^{N \times 128}$), defined as:

$$(\hat{\mathbf{v}}_t^\beta; \hat{\mathbf{v}}_t^\delta) = \text{MLP}(\mathcal{D}_{id}(\mathbf{H}_t)).\tag{4}$$

Pose Head with Amplitude Embeddings. To achieve precise and responsive control of jaw motion and head rotation, we extract frame-wise amplitude features \mathbf{A}_{amp} from the driving audio. Specifically, we first compute the amplitude envelope of the waveform and then apply frame-level window averaging to obtain a temporally aligned amplitude sequence that reflects speech intensity and rhythmic variations. These amplitude cues are injected into the pose branch via a cross-attention module \mathcal{D}_{pose} , where \mathbf{H}_t provides motion context and \mathbf{A}_{amp} provides audio-driven modulation.

The resulting features are decoded by an MLP to produce the velocity fields for jaw pose $\hat{\mathbf{v}}_t^{\theta^j} \in \mathbb{R}^{N \times 3}$ and global head rotation $\hat{\mathbf{v}}_t^{\theta^g} \in \mathbb{R}^{N \times 3}$:

$$(\hat{\mathbf{v}}_t^{\theta^j}, \hat{\mathbf{v}}_t^{\theta^g}) = \text{MLP}(\mathcal{D}_{pose}(\mathbf{H}_t, \mathbf{A}_{amp})).\tag{5}$$

Expression Head with Emotion Embeddings. To enable emotionally coherent facial expressions, we extract frame-wise emotion embeddings \mathbf{A}_{emo} from the driving audio using emotion2vec [48]. These embeddings capture subtle affective cues (e.g., happiness, sadness, anger) embedded in speech and are temporally aligned with the latent representation. The expression head injects \mathbf{A}_{emo} into the motion representation via a cross-attention module \mathcal{D}_{exp} , followed by a MLP that predicts the expression velocity field $\hat{\mathbf{v}}_t^\psi \in \mathbb{R}^{N \times 50}$, represented as:

$$\hat{\mathbf{v}}_t^\psi = \text{MLP}(\mathcal{D}_{exp}(\mathbf{H}_t, \mathbf{A}_{emo})).\tag{6}$$

Flow-matching Inference. During inference, the velocity fields from all heads are concatenated ($\hat{\mathbf{v}}_t = \text{Concat}(\hat{\mathbf{v}}_t^\beta, \hat{\mathbf{v}}_t^\psi, \hat{\mathbf{v}}_t^{\theta^j}, \hat{\mathbf{v}}_t^{\theta^g})$) to form a unified displacement field ε_t , which is iteratively updated to T_{inf} steps. The final FLAME parameters are obtained by adding this displacement to the reference:

$$\hat{\mathbf{X}} = \mathbf{X}_{ref} + \varepsilon_{T_{inf}}, \quad \varepsilon_t = \varepsilon_{t-1} + 1/T_{inf} \times \hat{\mathbf{v}}_t.\tag{7}$$

Flow-matching Training. During training, we model the continuous evolution of FLAME parameters as a straight flow between the initial latent ε_0 and the target displacement $\mathbf{X}_\Delta = \mathbf{X} - \mathbf{X}_{ref}$. Given a randomly sampled $t \sim \mathcal{U}(0, 1)$, the target velocity is defined as the linear interpolant, and the flow matching objective supervises the model-predicted velocity $\hat{\mathbf{v}}(t)$ as follows:

$$\mathcal{L}_{flow} = \mathbb{E}_{t \sim \mathcal{U}(0,1)} \left[\left\| \hat{\mathbf{v}}(t) - (t \mathbf{X}_\Delta + (1-t) \varepsilon_0) \right\|_2^2 \right].\tag{8}$$

This formulation directly aligns the model with the continuous flow that transports the latent state to the parameter space, enabling stable and temporally smooth synthesis. These designs allow 3DXTalker to achieve identity consistency, accurate lip synchronization, rich emotional expressions, and natural head motion within a unified framework.

3.3 Inference-Time Dynamic Controllability

Although the above pipeline generates natural and expressive motion, the outputs are largely driven by audio, offering limited global control over emotional intensity and spatial dynamics. To address this, we introduce two plug-in controllability modules: global emotion scaling and center motion control, enabling flexible style modulation at inference time.

Global Emotion Scalability. Benefiting from the disentanglement of shape and expression parameters in the FLAME model, we construct expression templates $\{\bar{\psi}^e\}_{e=1}^7$ from the MEAD dataset, covering seven emotional styles: Angry, Contempt, Disgust, Fear, Happy, Sad, and Surprise. Each template is associated with a template weight $\alpha \in \{1, 1.2, 1.4, 1.6, 1.8, 2.0\}$ that controls its intrinsic emotional intensity. During inference, we adjust the global emotional tone by interpolating between the reference expression ψ_{ref} and the scaled emotion template:

$$\hat{\psi}_{ref}^e = (1 - \lambda) \psi_{ref} + \lambda \alpha_e \bar{\psi}^e.\tag{9}$$

Table 1: Quantitative evaluation with seven baseline models over 200 videos. “ID Gen.” denotes whether the model supports identity-referred generalization. Our method achieves better performance on 3D-related metrics, demonstrating improved geometric accuracy and temporal coherence, while it performs well on most 2D perceptual metrics. The BA score assesses the rhythmic alignment of head motions with the driving audio. The MR is computed based on voting results from 74 voting responses. Throughput was measured on an NVIDIA RTX 5090 GPU. The **best** results are highlighted in bold and the second-best results are underlined.

| Model | Prediction Type | Identity | | | Lip-Sync | | | Expression | | | Pose BA | User Study MR | Efficiency Throughput (FPS) ↑ |
|--------------|-----------------|----------|-----------------------------------|-----------------|-----------------------------------|-----------------|-------------------|------------------------------------|------------------------------------|----------------------|--------------|---------------|-------------------------------|
| | | ID Gen. | MVE $(\times 10^{-3}) \downarrow$ | CSIM \uparrow | LVE $(\times 10^{-4}) \downarrow$ | LSEC \uparrow | LSED \downarrow | UFVE $(\times 10^{-3}) \downarrow$ | UFDD $(\times 10^{-4}) \downarrow$ | Emo-Fid \downarrow | | | |
| | | | | | | | | | | | | | |
| FaceFormer | Vert | ✗ | 4.704 | 0.919 | 1.801 | 0.751 | 13.584 | 4.094 | 4.970 | 0.351 | 0 | 4.46 | <u>74.640</u> |
| CodeTalker | Vert | ✗ | 4.795 | 0.920 | 1.886 | 0.777 | 13.311 | 4.123 | 3.783 | 0.374 | 0 | 4.63 | 64.997 |
| SelfTalk | Vert | ✗ | 4.803 | 0.921 | 1.863 | 0.843 | 13.385 | 4.106 | 3.659 | <u>0.336</u> | 0 | 4.45 | 9.083 |
| FaceDiffuser | Vert | ✗ | 4.752 | <u>0.933</u> | 1.624 | 0.636 | 12.732 | 4.173 | 3.567 | 0.398 | 0 | 4.58 | 16.142 |
| EMOTE | Para | ✗ | 2.883 | 0.896 | 1.539 | <u>2.706</u> | 13.488 | 2.615 | <u>2.974</u> | 0.359 | 0 | 4.45 | 91.417 |
| DEEPTalk | Para | ✗ | <u>2.672</u> | 0.915 | <u>1.535</u> | 2.174 | 13.564 | <u>2.306</u> | 3.146 | 0.355 | 0 | <u>4.28</u> | 59.604 |
| DiffPoseTalk | Para | ✗ | 2.877 | 0.876 | 1.698 | 4.021 | <u>13.069</u> | 2.453 | 3.187 | 0.377 | <u>0.338</u> | 4.94 | 18.795 |
| Ours | Para | ✓ | 1.371 | 0.967 | 0.877 | 1.674 | 13.330 | 1.113 | 1.317 | 0.259 | 0.404 | 4.22 | 69.497 |

This provides seven types of global emotion control, each with six levels, while preserving the audio-driven, nuanced expression dynamics. (Details in [Appendix E.1](#).)

Head-Pose Motion Control. While the predicted mesh sequences exhibit natural but subtle head sway, they lack explicit controllability over head-pose motion. To enhance head presence while preserving realism, we introduce a head-pose control module that provides high-level, interpretable control over head motion. Given the driving audio or a text prompt describing the desired presentation style, a language model generates a simple head-pose trajectory in the form of smooth and interpretable control functions (e.g., gentle sways, rhythmic arcs, or gradual rotations). Rather than replacing the original motion, the generated trajectory is superimposed onto the model-predicted natural head dynamics, yielding controllable yet realistic head-pose motion. This design enables flexible stylistic variation—such as calm, energetic, or stage-presenting delivery—while preserving identity consistency and expression dynamics. Prompt details are provided in [Appendix H](#).

4 Experiments

4.1 Implementation Details

Baselines. We compare our 3DXTalker with seven competitive baselines, including (1) FaceFormer [5]; (2) CodeTalker [44]; (3) SelfTalk [40]; (4) DiffPoseTalk [11]; (5) EMOTE [8]; (6) FaceDiffuser [46]; (7) DEEPTalk [10].

Datasets. We train models on six diverse talking-head datasets, including lab-scanned (GRID [25], RAVDESS [26], MEAD [27]) and in-the-wild sources (CelebV-HQ [30], HDTF [29], and VoxCeleb2 [28]), covering over 11.7k cleaned audio-video pairs with an average of over 15 seconds. We evaluate models on 200 video cases, each with a fixed duration of 10 seconds. More details are in [Appendix B.1](#).

Setup. The Transformer backbone uses 6 blocks with a hidden size of 768, where each prediction branch has 2 blocks. 3DXTalker is trained for 100 epochs with batch size of 128 and frame size of 250 on two NVIDIA H100 GPUs using AdamW (learning rate 1×10^{-4} , weight decay 0.01) with OneCycleLR scheduler. Flow-matching steps are set to 512 for training and 32 for inference. Implementation details are provided in [Appendix B.2](#).

Metrics. We evaluate 3DXTalker over 9 metrics across four dimensions. Identity preservation is measured by MVE [15], and CSIM [49], where MVE captures the 3D geometric error between predicted and ground-truth meshes, and CSIM computes frame-wise embedding similarity to ensure identity consistency in 2D appearance. Lip synchronization is assessed using LVE [5], LSEC and LSED [50]; LVE measures 3D vertex-level lip alignment, while LSEC and LSED quantify audio-2D visual sync quality through confidence and embedding-distance mismatch. Facial expression quality is evaluated using UFVE [46], UFDD [44], and Emo-FID [10]; UFVE measures 3D upper-face geometry errors, UFDD examines 3D temporal smoothness of expression dynamics, and Emo-FID reflects 2D facial expression similarities. Head-pose motion is measured using beat alignment (BA) score [11, 51]. Besides, we evaluate perceptual quality via a subjective User Study, reporting the mean rank (MR) based on participant preferences. Finally, FPS is recorded during inference for efficiency evaluation. We compute 3D metrics on meshes and 2D metrics on rendered videos. Details are in [Appendix B.3](#).

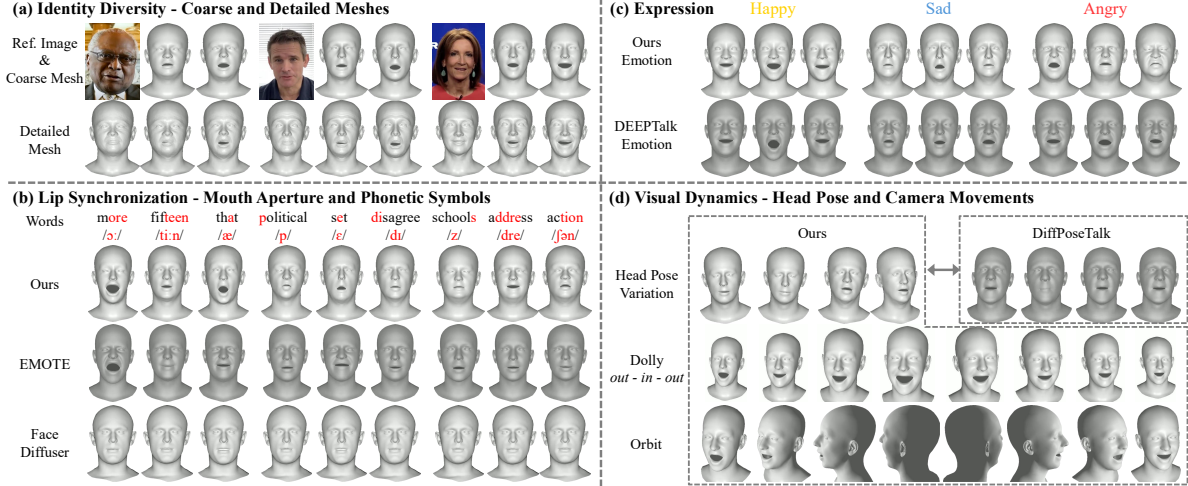


Figure 3: Qualitative comparisons over selected typical baselines. (a) shows the consistency between generated meshes and the reference image. (b) shows better mouth aperture alignment. (c) shows finer emotional expressiveness. (d) shows predicted natural head pose and camera movements. Full baseline comparisons are provided in **Appendix C**. Other emotion comparisons are offered in **Appendix E.2**

Table 2: Ablation results of 3DXTalker. “AbsLatent” uses absolute latent instead of differential ones in Eq. (2). “w/o \mathbf{A}_{emo} ” and “w/o \mathbf{A}_{amp} ” remove emotional and amplitude embeddings, respectively. The best results in **bold** and second-best underlined.

| Model | LVE ($\times 10^{-4}$) \downarrow | MVE ($\times 10^{-3}$) \downarrow | UFDD ($\times 10^{-4}$) \downarrow | UFVE ($\times 10^{-3}$) \downarrow | LSEC \uparrow | LSED \downarrow | CSIM \uparrow |
|------------------------|--|--|---|---|--------------------|----------------------|--------------------|
| AbsLatent | 1.242 | 1.558 | 1.479 | 1.212 | 1.794 | <u>13.348</u> | 0.959 |
| w/o \mathbf{A}_{amp} | 0.971 | 1.417 | <u>1.328</u> | <u>1.133</u> | 0.240 | 14.116 | 0.975 |
| w/o \mathbf{A}_{emo} | <u>0.926</u> | <u>1.414</u> | 1.373 | 1.142 | 1.308 | 13.425 | 0.966 |
| Ours | 0.877 | 1.371 | 1.317 | 1.113 | <u>1.674</u> | 13.330 | <u>0.967</u> |

4.2 Main Results

Quantitative Evaluation. We quantitatively compare our method with seven competitive baselines across identity, lip sync, emotional expression, head pose, and efficiency, listed in Table 1. Our method performs well across the 3D-related metrics (MVE, LVE, UFVE, UFDD), suggesting accurate geometry reconstruction and stable temporal motion compared to the evaluated baselines. For 2D perceptual metrics, 3DXTalker attains competitive results on CSIM and Emo-FID, indicating consistent identity preservation and credible affective quality. The Lip-sync performance is strong overall, while LSEC and LSED remain challenging. We note that most 3D-based methods exhibit similarly limited improvements on these phoneme-sensitive metrics, except for FaceDiffuser. The BA score demonstrates that 3DXTalker can generate head-pose motions that are rhythmically synchronized with the input audio. User study shows that 3DXTalker achieves the best Mean Rank of 4.22, reflecting a human preference for its overall perceptual quality and naturalness compared to the baselines. Finally, 3DXTalker achieves reasonable inference at 69.497 FPS. These results collectively validate that 3DXTalker has strong potential for expressive generation, achieving a balanced trade-off between performance and efficiency.

Qualitative Evaluation. Figure 3 provides qualitative comparisons against several representative baselines (Full comparisons are presented in the **Appendix C**). As shown in Figure 3 (a), 3DXTalker effectively preserves identity while observing shapes and details, producing meshes that closely match the reference image. In Figure 3 (b), our method achieves clearer mouth aperture alignment across diverse word syllables, demonstrating a tighter correspondence between mouth movements and speech. Figure 3 (c) highlights the model’s ability to generate finer emotional expressions, capturing subtle variations in facial dynamics as the speech evolves. Finally, Figure 3 (d) illustrates natural head-pose behaviors along with different camera movements generated by our 3DXTalker. Overall, these results show that 3DXTalker can synthesize diverse, dynamic, and expressive 3D talking videos.

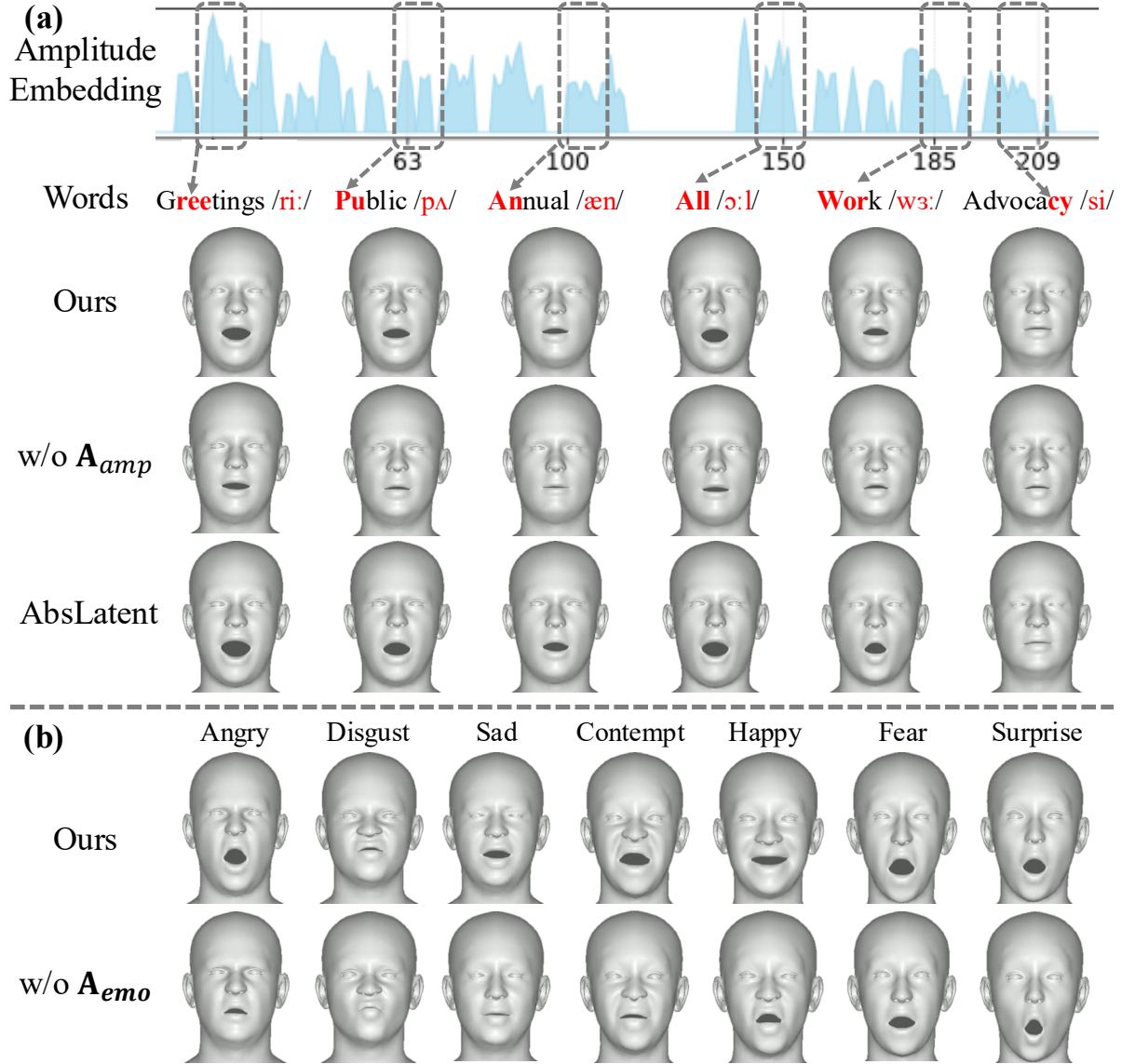


Figure 4: Visualizations of ablation results from Table 2. (a) is conducted on the same audio. (b) extracts each emotion from corresponding videos at the same frame. Details in **Appendix D**.

4.3 Ablation Study

We conduct ablation experiments to evaluate the contribution of key components in 3DXTalker, with quantitative results listed in Table 2 and visual comparisons shown in Figure 4. Using absolute latent leads to the largest 3D errors and lower CSIM identity scores, indicating that our differential latent design in the dataset-curation pipeline helps separate identity from motion and is important to stable motion generation. Removing A_{amp} increases CSIM as it reduces mouth-motion variation, which artificially enhances frame similarity (Figure 4 (a)). It also leads to higher 3D errors, confirming that amplitude cues provide essential constraints on realistic mouth aperture. Likewise, removing A_{emo} degrades 3D performance across all geometric metrics and disrupts subtle emotional expression (Figure 4 (b)), underscoring the importance of frame-wise emotion features. These findings validate our incorporation of frame-wise amplitude and emotion cues, forming audio-rich representations that strengthen speech-driven facial motions.

4.4 Analysis

Global Emotion Scalability. To further examine the model’s emotion controllability, we compute cosine similarity across seven emotions in the FLAME expression space, as listed in Table 3. 3DXTalker consistently achieves higher

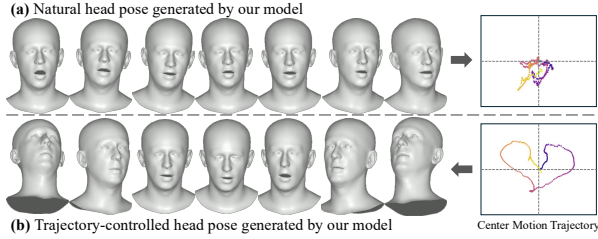


Figure 5: Our 3DXTalker supports two head-pose modes: (a) natural micro-movements learned from in-the-wild data, and (b) controllable head dynamics (with natural micro-movements) guided by a center motion trajectory. Trajectory colors indicate temporal progression (dark→light). See **Appendix F** for more examples.

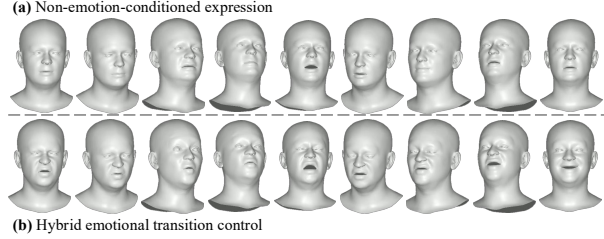


Figure 6: 3DXTalker supports emotion control and seamless transitions between facial expressions. (a) shows the neutral talking-face state without guided emotion intervention, and (b) enables multiple emotion transitions among five emotion categories (angry → surprised → sad → contempt → happy).

Table 3: Emotion-wise cosine similarity between generated and ground-truth FLAME expression parameters. “ E_C ” denotes emotion control. Ang. = Angry, Con. = Contempt, Dis. = Disgust, Fea. = Fear, Hap. = Happy, Sad = Sad, Sur. = Surprise. Mesh visualization and analyses are provided in **Appendix E**.

| Model | Ang. | Con. | Dis. | Fea. | Hap. | Sad | Sur. |
|------------------|-------|-------|-------|-------|-------|-------|-------|
| DEEPTalk + E_C | 0.637 | 0.738 | 0.602 | 0.686 | 0.721 | 0.659 | 0.640 |
| Ours + E_C | 0.947 | 0.935 | 0.953 | 0.933 | 0.921 | 0.939 | 0.938 |

similarity scores than DEEPTalk, demonstrating superior emotion controllability and coherence. Figure 6 shows temporal emotion controllability. In Figure 6(a) Without explicit emotion conditioning control, the generated talking head stays near a neutral state with limited affective variation. In contrast, Figure 6(b) shows that our hybrid transition control enables smooth, flicker-free transitions across multiple emotion categories while preserving identity-consistent geometry, indicating that the control signal modulates expression in a structured and continuous manner. Moreover, we further present a t-SNE visualization of our expression predictions in **Appendix E**. Partial overlaps between angry–disgust and surprise–fear are observed due to their similar facial activation patterns, while other clusters remain well separated, indicating that our model captures meaningful structure in the FLAME expression space.

Pose Analysis. We further analyze both jaw and head pose predictions. For jaw pose (Figure 7), the predicted jaw-opening pose (θ_0^j) trajectories with two individual seeds exhibit temporal consistency with the ground truth and closely follow the audio-amplitude, demonstrating that amplitude conditioning effectively contributes to mouth aperture. Regarding head pose (Figure 5), 3DXTalker maintains high stability and continuity across both supported modes. The results demonstrate that the model achieves both realistic pose generation and scalable, user-controllable dynamics without introducing abrupt jitter or pose discontinuities.

5 Conclusion

In summary, we present **3DXTalker**, a comprehensive framework for expressive audio-driven 3D talking avatar generation that jointly advances identity modeling, audio expressiveness, and controllable dynamics. By constructing a scalable 2D-to-3D data-curated identity modeling pipeline with disentangled representations, 3DXTalker enables robust generalization across diverse speaker identities without relying on costly 3D capture. Moreover, by introducing audio-rich representations that explicitly capture frame-wise amplitude and emotional cues, our method achieves accurate lip synchronization and nuanced emotional expression. Combined with controllable head-pose modulation built upon natural motion priors, 3DXTalker produces identity-consistent, lip-synchronized, emotionally expressive, and spatially dynamic 3D talking avatars within a unified paradigm. Overall, our results demonstrate the effectiveness of the proposed formulation and highlight a practical path toward holistic expressivity in next-generation avatar systems. We believe that 3DXTalker provides a flexible and extensible foundation for future research on expressive digital humans, as well as broader applications in virtual communication and digital content creation.

References

[1] Wojciech Zienonka, Timo Bolkart, and Justus Thies. Instant volumetric head avatars, 2023.

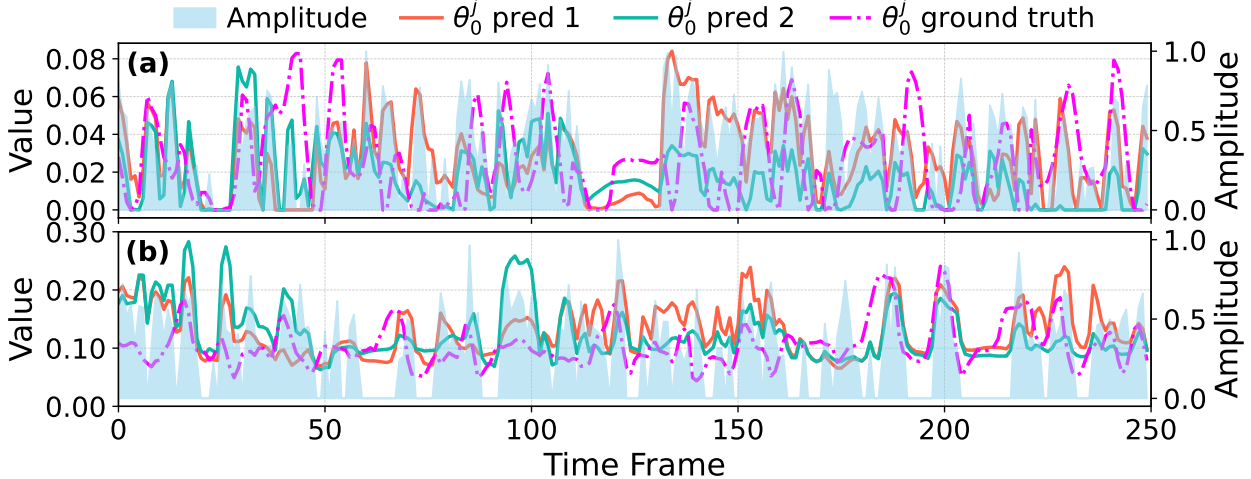


Figure 7: Curves for the ground truth and two predicted sequences, showing correlation with the amplitude-driven mouth aperture.

- [2] Linchao Bao, Xiangkai Lin, Yajing Chen, Haoxian Zhang, Sheng Wang, Xuefei Zhe, Di Kang, Haozhi Huang, Xinwei Jiang, Jue Wang, Dong Yu, and Zhengyou Zhang. High-fidelity 3d digital human head creation from rgb-d selfies, 2021.
- [3] Jun Yu and Chang Wen Chen. From talking head to singing head: A significant enhancement for more natural human computer interaction. In *2017 IEEE International Conference on Multimedia and Expo (ICME)*, pages 511–516, 2017.
- [4] Jiahe Li, Jiawei Zhang, Xiao Bai, Jin Zheng, Jun Zhou, and Lin Gu. Instag: Learning personalized 3d talking head from few-second video, 2025.
- [5] Yingruo Fan, Zhaojiang Lin, Jun Saito, Wenping Wang, and Taku Komura. Faceformer: Speech-driven 3d facial animation with transformers. In *Proceedings of the IEEE/CVF Conference on Computer Vision and Pattern Recognition (CVPR)*, 2022.
- [6] Daniel Cudeiro, Timo Bolkart, Cassidy Laidlaw, Anurag Ranjan, and Michael Black. Capture, learning, and synthesis of 3D speaking styles. *Computer Vision and Pattern Recognition (CVPR)*, pages 10101–10111, 2019.
- [7] Alexander Richard, Michael Zollhöfer, Yandong Wen, Fernando de la Torre, and Yaser Sheikh. Meshtalk: 3d face animation from speech using cross-modality disentanglement. In *Proceedings of the IEEE/CVF International Conference on Computer Vision (ICCV)*, pages 1173–1182, October 2021.
- [8] Radek Daněček, Kiran Chhatre, Shashank Tripathi, Yandong Wen, Michael Black, and Timo Bolkart. Emotional speech-driven animation with content-emotion disentanglement. In *SIGGRAPH Asia 2023 Conference Papers*, pages 1–13, 2023.
- [9] Ziqiao Peng, Haoyu Wu, Zhenbo Song, Hao Xu, Xiangyu Zhu, Jun He, Hongyan Liu, and Zhaoxin Fan. Emotalk: Speech-driven emotional disentanglement for 3d face animation, 2023.
- [10] Jisoo Kim, Jungbin Cho, Joonho Park, Soonmin Hwang, Da Eun Kim, Geon Kim, and Youngjae Yu. Deeptalk: Dynamic emotion embedding for probabilistic speech-driven 3d face animation, 2024.
- [11] Zhiyao Sun, Tian Lv, Sheng Ye, Matthieu Lin, Jenny Sheng, Yu-Hui Wen, Minjing Yu, and Yong-Jin Liu. Diffposetalk: Speech-driven stylistic 3d facial animation and head pose generation via diffusion models. *ACM Transactions on Graphics (TOG)*, 43(4), 2024.
- [12] Daniel Cudeiro, Timo Bolkart, Cassidy Laidlaw, Anurag Ranjan, and Michael J Black. Capture, learning, and synthesis of 3d speaking styles. In *Proceedings of the IEEE/CVF conference on computer vision and pattern recognition*, pages 10101–10111, 2019.
- [13] Cheng-hsin Wuu, Ningyuan Zheng, Scott Ardisson, Rohan Bali, Danielle Belko, Eric Brockmeyer, Lucas Evans, Timothy Godisart, Hyowon Ha, Xuhua Huang, et al. Multiface: A dataset for neural face rendering. 2022.
- [14] Gabriele Fanelli, Juergen Gall, Harald Romsdorfer, Thibaut Weise, and Luc Van Gool. A 3-d audio-visual corpus of affective communication. *IEEE Transactions on Multimedia*, 12(6):591–598, 2010.

[15] Xiangyu Fan, Jiaqi Li, Zhiqian Lin, Weiye Xiao, and Lei Yang. Unitalker: Scaling up audio-driven 3d facial animation through a unified model. In *European Conference on Computer Vision*, pages 204–221. Springer, 2024.

[16] Wei-Ning Hsu, Benjamin Bolte, Yao-Hung Hubert Tsai, Kushal Lakhotia, Ruslan Salakhutdinov, and Abdelrahman Mohamed. Hubert: Self-supervised speech representation learning by masked prediction of hidden units. *IEEE/ACM transactions on audio, speech, and language processing*, 29:3451–3460, 2021.

[17] Sanyuan Chen, Chengyi Wang, Zhengyang Chen, Yu Wu, Shujie Liu, Zhuo Chen, Jinyu Li, Naoyuki Kanda, Takuya Yoshioka, Xiong Xiao, et al. Wavlm: Large-scale self-supervised pre-training for full stack speech processing. *IEEE Journal of Selected Topics in Signal Processing*, 16(6):1505–1518, 2022.

[18] Alexei Baevski, Yuhao Zhou, Abdelrahman Mohamed, and Michael Auli. wav2vec 2.0: A framework for self-supervised learning of speech representations. *Advances in neural information processing systems*, 33:12449–12460, 2020.

[19] Yihong Lin, Zhaoxin Fan, Xianjia Wu, Lingyu Xiong, Liang Peng, Xiandong Li, Wenxiong Kang, Songju Lei, and Huang Xu. Glditalker: Speech-driven 3d facial animation with graph latent diffusion transformer. 2024.

[20] Shivangi Aneja, Justus Thies, Angela Dai, and Matthias Nießner. Facetalk: Audio-driven motion diffusion for neural parametric head models. In *Proceedings of the IEEE/CVF Conference on Computer Vision and Pattern Recognition*, pages 21263–21273, 2024.

[21] Sichun Wu, Kazi Injamamul Haque, and Zerrin Yumak. Probtalk3d: Non-deterministic emotion controllable speech-driven 3d facial animation synthesis using vq-vae. In *Proceedings of the 17th ACM SIGGRAPH Conference on Motion, Interaction, and Games*, MIG ’24, New York, NY, USA, 2024. Association for Computing Machinery.

[22] Yao Feng, Haiwen Feng, Michael J. Black, and Timo Bolkart. Learning an animatable detailed 3D face model from in-the-wild images. In *ACM Transactions on Graphics, (Proc. SIGGRAPH)*, volume 40, 2021.

[23] Radek Daněček, Michael J Black, and Timo Bolkart. Emoca: Emotion driven monocular face capture and animation. In *Proceedings of the IEEE/CVF Conference on Computer Vision and Pattern Recognition*, pages 20311–20322, 2022.

[24] Tianye Li, Timo Bolkart, Michael. J. Black, Hao Li, and Javier Romero. Learning a model of facial shape and expression from 4D scans. *ACM Transactions on Graphics, (Proc. SIGGRAPH Asia)*, 36(6):194:1–194:17, 2017.

[25] Martin Cooke, Jon Barker, Stuart Cunningham, and Xu Shao. An audio-visual corpus for speech perception and automatic speech recognition. *The Journal of the Acoustical Society of America*, 120(5):2421–2424, 2006.

[26] Steven R Livingstone and Frank A Russo. The ryerson audio-visual database of emotional speech and song (ravdess): A dynamic, multimodal set of facial and vocal expressions in north american english. *PloS one*, 13(5):e0196391, 2018.

[27] Kaisiyuan Wang, Qianyi Wu, Linsen Song, Zhuoqian Yang, Wayne Wu, Chen Qian, Ran He, Yu Qiao, and Chen Change Loy. Mead: A large-scale audio-visual dataset for emotional talking-face generation. In *ECCV*, 2020.

[28] Joon Son Chung, Arsha Nagrani, and Andrew Zisserman. Voxceleb2: Deep speaker recognition. In *Interspeech 2018*, pages 1086–1090, 2018.

[29] Zhimeng Zhang, Lincheng Li, Yu Ding, and Changjie Fan. Flow-guided one-shot talking face generation with a high-resolution audio-visual dataset. In *Proceedings of the IEEE/CVF conference on computer vision and pattern recognition*, pages 3661–3670, 2021.

[30] Hao Zhu, Wayne Wu, Wentao Zhu, Liming Jiang, Siwei Tang, Li Zhang, Ziwei Liu, and Chen Change Loy. CelebV-HQ: A large-scale video facial attributes dataset. In *ECCV*, 2022.

[31] James Booth, Anastasios Roussos, Stefanos Zafeiriou, Allan Ponniah, and David Dunaway. A 3d morphable model learnt from 10,000 faces. In *Proceedings of the IEEE conference on computer vision and pattern recognition*, pages 5543–5552, 2016.

[32] Thomas Gerig, Andreas Morel-Forster, Clemens Blumer, Bernhard Egger, Marcel Luthi, Sandro Schoenborn, and Thomas Vetter. Morphable face models - an open framework. In *2018 13th IEEE International Conference on Automatic Face & Gesture Recognition (FG 2018)*, pages 75–82, 2018.

[33] Panagiotis P. Filntisis, George Retsinas, Foivos Paraperas-Papantonio, Athanasios Katsamanis, Anastasios Roussos, and Petros Maragos. Visual speech-aware perceptual 3d facial expression reconstruction from videos. 2022.

[34] Wojciech Zielenka, Timo Bolkart, and Justus Thies. Towards metrical reconstruction of human faces. In *ECCV*, 2022.

[35] Ziqiao Peng, Yanbo Fan, Haoyu Wu, Xuan Wang, Hongyan Liu, Jun He, and Zhaoxin Fan. Dualtalk: Dual-speaker interaction for 3d talking head conversations. In *Proceedings of the IEEE/CVF Conference on Computer Vision and Pattern Recognition*, 2025.

[36] Yixiang Zhuang, Chunshan Ma, Yao Cheng, Xuan Cheng, Jing Liao, and Juncong Lin. Talkingeyes: Pluralistic speech-driven 3d eye gaze animation. 2025.

[37] Xinmu Wang, Xiang Gao, Xiyun Song, Heather Yu, Zongfang Lin, Liang Peng, and Xianfeng Gu. Ot-talk: Animating 3d talking head with optimal transportation. In *Proceedings of the 2025 International Conference on Multimedia Retrieval*, pages 1340–1349, 2025.

[38] Xuangeng Chu, Nabarun Goswami, Ziteng Cui, Hanqin Wang, and Tatsuya Harada. Artalk: Speech-driven 3d head animation via autoregressive model. 2025.

[39] Federico Nocentini, Thomas Besnier, Claudio Ferrari, Sylvain Arguillere, Stefano Berretti, and Mohamed Daoudi. Scantalk: 3d talking heads from unregistered scans. In *European Conference on Computer Vision*, pages 19–36. Springer, 2024.

[40] Ziqiao Peng, Yihao Luo, Yue Shi, Hao Xu, Xiangyu Zhu, Hongyan Liu, Jun He, and Zhaoxin Fan. Selftalk: A self-supervised commutative training diagram to comprehend 3d talking faces. In *Proceedings of the 31st ACM International Conference on Multimedia*, pages 5292–5301, 2023.

[41] Sunjin Jung, Sewhan Chun, and Junyong Noh. Audio-Driven Speech Animation with Text-Guided Expression. In Renjie Chen, Tobias Ritschel, and Emily Whiting, editors, *Pacific Graphics Conference Papers and Posters*. The Eurographics Association, 2024.

[42] Evonne Ng, Hanbyul Joo, Liwen Hu, Hao Li, Trevor Darrell, Angjoo Kanazawa, and Shiry Ginosar. Learning to listen: Modeling non-deterministic dyadic facial motion. In *Proceedings of the IEEE/CVF Conference on Computer Vision and Pattern Recognition (CVPR)*, pages 20395–20405, June 2022.

[43] Kim Sung-Bin, Lee Hyun, Da Hye Hong, Suekyeong Nam, Janghoon Ju, and Tae-Hyun Oh. Laughtalk: Expressive 3d talking head generation with laughter. 2023.

[44] Jinbo Xing, Menghan Xia, Yuechen Zhang, Xiaodong Cun, Jue Wang, and Tien-Tsin Wong. Codetalker: Speech-driven 3d facial animation with discrete motion prior. In *Proceedings of the IEEE/CVF Conference on Computer Vision and Pattern Recognition*, pages 12780–12790, 2023.

[45] Kang Shen, Haifeng Xia, Guangxing Geng, Guangyue Geng, Siyu Xia, and Zhengming Ding. Deitalk: Speech-driven 3d facial animation with dynamic emotional intensity modeling. In *Proceedings of the 32nd ACM International Conference on Multimedia*, pages 10506–10514, 2024.

[46] Stefan Stan, Kazi Injamamul Haque, and Zerrin Yumak. Facediffuser: Speech-driven 3d facial animation synthesis using diffusion. In *Proceedings of the 16th ACM SIGGRAPH Conference on Motion, Interaction and Games*, pages 1–11, 2023.

[47] Peng Chen, Xiaobao Wei, Ming Lu, Yitong Zhu, Naiming Yao, Xingyu Xiao, and Hui Chen. Diffusiontalker: Personalization and acceleration for speech-driven 3d face diffuser. 2023.

[48] Ziyang Ma, Zhisheng Zheng, Jiaxin Ye, Jinchao Li, Zhifu Gao, Shiliang Zhang, and Xie Chen. emotion2vec: Self-supervised pre-training for speech emotion representation. *Proc. ACL 2024 Findings*, 2024.

[49] Safouane El Ghazouali, Umberto Michelucci, Yassin El Hillali, and Hichem Nouira. Csim: A copula-based similarity index sensitive to local changes for image quality assessment, 2024.

[50] KR Prajwal, Rudrabha Mukhopadhyay, Vinay P Namboodiri, and CV Jawahar. A lip sync expert is all you need for speech to lip generation in the wild. In *Proceedings of the 28th ACM international conference on multimedia*, pages 484–492, 2020.

[51] Li Siyao, Weijiang Yu, Tianpei Gu, Chunze Lin, Quan Wang, Chen Qian, Chen Change Loy, and Ziwei Liu. Bailando: 3d dance generation via actor-critic gpt with choreographic memory. In *CVPR*, 2022.

[52] Alec Radford, Jong Wook Kim, Tao Xu, Greg Brockman, Christine McLeavey, and Ilya Sutskever. Robust speech recognition via large-scale weak supervision, 2022.

[53] J. S. Chung and A. Zisserman. Out of time: automated lip sync in the wild. In *Workshop on Multi-view Lip-reading, ACCV*, 2016.

[54] Tanneru. Beit-large fine-tuned on affectnet for emotion detection, 2025.

[55] Shivangi Aneja, Justus Thies, Angela Dai, and Matthias Nießner. Facetalk: Audio-driven motion diffusion for neural parametric head models, 2024.

[56] Team Wan, Ang Wang, Baole Ai, Bin Wen, Chaojie Mao, Chen-Wei Xie, Di Chen, Feiwu Yu, Haiming Zhao, Jianxiao Yang, Jianyuan Zeng, Jiayu Wang, Jingfeng Zhang, Jingren Zhou, Jinkai Wang, Jixuan Chen, Kai Zhu, Kang Zhao, Keyu Yan, Lianghua Huang, Mengyang Feng, Ningyi Zhang, Pandeng Li, Pingyu Wu, Ruihang Chu, Ruili Feng, Shiwei Zhang, Siyang Sun, Tao Fang, Tianxing Wang, Tianyi Gui, Tingyu Weng, Tong Shen, Wei Lin, Wei Wang, Wei Wang, Wenmeng Zhou, Wente Wang, Wenting Shen, Wenyuan Yu, Xianzhong Shi, Xiaoming Huang, Xin Xu, Yan Kou, Yangyu Lv, Yifei Li, Yijing Liu, Yiming Wang, Yingya Zhang, Yitong Huang, Yong Li, You Wu, Yu Liu, Yulin Pan, Yun Zheng, Yuntao Hong, Yupeng Shi, Yutong Feng, Zeyinzi Jiang, Zhen Han, Zhi-Fan Wu, and Ziyu Liu. Wan: Open and advanced large-scale video generative models. *arXiv preprint arXiv:2503.20314*, 2025.

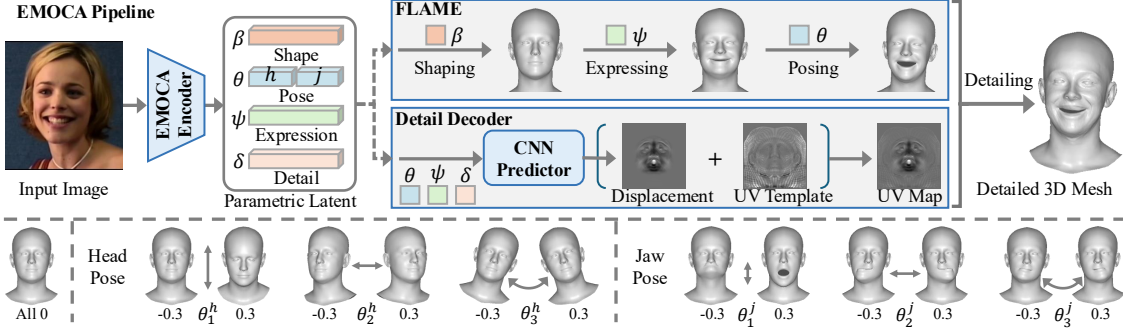


Figure 8: EMOCA modeling pipeline using the FLAME model. The encoder outputs parametric latent codes: β for facial shape, ψ for expression, θ for head pose and jaw pose dynamics, and δ for fine-grained appearance details (e.g., texture). We linearly vary θ to demonstrate controllable changes in head and jaw pose, as illustrated in the bottom row.

A EMOCA Modeling Preliminary

To leverage the abundant identities, emotional styles, and dynamic motion patterns available in large-scale 2D video data, we adopt the EMOCA parametric autoencoder [23], which lifts individual video frames into a controllable 3D facial parameter space, as illustrated in Figure 8. This formulation allows us to effectively bridge the gap between rich 2D visual observations and structured 3D facial representations, enabling scalable identity and motion modeling without relying on explicit 3D capture.

Specifically, the model encodes each 2D image into a set of FLAME parameters [24], including the identity-dependent shape $\beta \in \mathbb{R}^{100}$, head pose $\theta \in \mathbb{R}^6$, facial expression $\psi \in \mathbb{R}^{50}$, as well as an additional detail parameter $\delta \in \mathbb{R}^{128}$ that captures high-frequency facial geometry. These parameters are then decoded into a coarse facial mesh $\mathbf{M}_{coa} \in \mathbb{R}^{5023 \times 3}$ by deforming the FLAME template $\bar{\mathbf{V}}$ according to β , ψ , and θ . Finally, the coarse mesh is further refined by a detail decoder \mathcal{D}_{det} , which applies a facial displacement map to generate a high-resolution mesh $\mathbf{M}_{det} \in \mathbb{R}^{59315 \times 3}$, formally defined as:

$$\begin{aligned} \mathbf{V}_{int} &= \bar{\mathbf{V}} + \mathbf{B}_S(\beta) + \mathbf{B}_E(\psi), \\ \mathbf{M}_{coa} &= \text{LBS}(\mathbf{V}_{int}, \mathbf{J}_P(\bar{\mathbf{V}}), \mathcal{W}, \theta), \\ \mathbf{M}_{det} &= \mathbf{F}_{det}(\mathbf{M}_{coa}, (\bar{\mathbf{U}} + \mathcal{D}_{det}(\theta, \psi, \delta))), \end{aligned} \quad (10)$$

where \mathbf{V}_{int} denotes an intermediate mesh representation, \mathbf{B}_S and \mathbf{B}_E are the shaping and expression blend functions, respectively, and LBS refers to the linear blend skinning operation parameterized by the joint regressors \mathbf{J}_P and the skinning weights \mathcal{W} . The template UV map is represented by $\bar{\mathbf{U}}$, and \mathbf{F}_{det} applies the predicted facial displacement map to the coarse mesh \mathbf{M}_{coa} , refining it into a detailed surface geometry. Notably, the pose parameter θ can be naturally decomposed into *head pose* and *jaw pose*, enabling head motion to be modeled and manipulated independently from facial articulation through simple linear variations in the pose space. This separation facilitates explicit and interpretable control over global head dynamics without interfering with lip and expression movements. Overall, this parameterization yields a disentangled and physically meaningful 3D facial representation, which forms the foundation of our subsequent data-curated identity modeling pipeline and supports scalable learning across diverse identities, expressions, and motion patterns.

B Implementation Details

B.1 Dataset Curation Pipeline Details

To address the scarcity of training data and limited identity diversity in 3D talking avatar generation, we construct a large-scale corpus by integrating six diverse 2D video datasets. Specifically, we collect six widely used 2D talking video datasets, including three lab-controlled datasets (GRID [25], RAVDESS [26], MEAD [27]) and three in-the-wild datasets (VoxCeleb2 [28], HDTF [29], CelebV-HQ [30]). The lab-controlled datasets provide high-quality recordings with articulated facial movements and emotional expressions, while the in-the-wild datasets introduce a broad range of identities, speaking styles, and natural head pose dynamics. To ensure consistency and quality across these sources, we apply a unified data preprocessing pipeline to filter outliers, following the steps below:

- (1) **Duration Filtering.** Lab-controlled datasets contain high-quality recordings with rich expressions but are limited by short clip lengths (3–5 seconds). To facilitate temporal modeling, we concatenate clips sharing the

Table 4: Statistics of the curated talking video dataset after our data curation pipeline.

| Dataset | ID | Environment | Year | Raw Resolution | Size | Subject | Total Duration (s) | Hours (h) | Avg. Duration (s/sample) |
|-----------|----|-------------|------|----------------|------|---------|--------------------|-----------|--------------------------|
| GRID | V0 | Lab | 2006 | 720 × 576 | 6600 | 34 | 99257.81 | 27.57 | 15.04 |
| RAVDESS | V1 | Lab | 2018 | 1280 × 1024 | 613 | 24 | 10071.88 | 2.80 | 16.43 |
| MEAD | V2 | Lab | 2020 | 1920 × 1080 | 1969 | 60 | 42868.77 | 11.91 | 21.77 |
| VoxCeleb2 | V3 | Wild | 2018 | 360P~720P | 1326 | 1k+ | 21528.20 | 5.98 | 16.24 |
| HDTF | V4 | Wild | 2021 | 720P~1080P | 400 | 300+ | 55452.08 | 15.40 | 138.63 |
| Celebv-HQ | V5 | Wild | 2022 | 512 × 512 | 798 | 700+ | 13486.20 | 3.75 | 16.90 |

Table 5: Dataset split for training and test.

| Dataset | ID | Total Size | Training Set | Test Set |
|-----------|----|------------|--------------|----------|
| GRID | V0 | 6600 | 6570 | 30 |
| RAVDESS | V1 | 613 | 583 | 30 |
| MEAD | V2 | 1969 | 1939 | 30 |
| VoxCeleb2 | V3 | 1326 | 1996 | 30 |
| HDTF | V4 | 400 | 350 | 50 |
| Celebv-HQ | V5 | 798 | 768 | 30 |
| Summary | | 11706 | 11506 | 200 |

same identity and emotion, yielding sequences of approximately 10–20 seconds. In contrast, as in-the-wild datasets typically feature longer durations, we simply filter out samples shorter than 10 seconds.

- (2) **Signal-to-Noise Ratio Filtering.** To remove clips compromised by strong background noise, music, or environmental interference, we compute the signal-to-noise ratio (SNR) for each audio segment, discarding samples with SNR below a predefined threshold. This step is critical for in-the-wild datasets, where recordings often contain crowd noise, reverberation, or microphone artifacts. The SNR filtering of speech signals ensures reliable cues for reliable amplitude extraction, emotion inference, and audio–visual synchronization.
- (3) **Language Filtering.** We enforce linguistic consistency by filtering clips based on spoken language using Whisper [52], discarding non-English samples or those with low detection confidence. This filtering step prevents mixing heterogeneous phonetic structures and prosodic patterns, reducing potential interference with audio–visual alignment.
- (4) **Audio-Visual Sync Filtering.** To guarantee strict audio–visual alignment, we filter samples using SyncNet [53] to evaluate the temporal correlation between lip motion and the speech signal. We discard clips exhibiting high synchronization errors, as well as those containing abrupt scene cuts or off-screen speakers (e.g., voice-overs). Eliminating these misaligned pairs is essential, as they provide incorrect supervision signals that can significantly degrade lip-sync learning and hinder expression modeling.
- (5) **Resolution Normalization.** To ensure visual resolution across diverse datasets, each video is first resized by matching its shorter side to 512 pixels while preserving aspect ratio, followed by a center crop to obtain frames at a unified resolution of 512 × 512. After cropping, all videos are re-encoded at 25 FPS with standardized RGB for consistent motion sampling. This normalization step harmonizes data from sources with varying aspect ratios, camera qualities, and spatial resolutions.

After the above preprocessing steps, we obtain a high-quality talking video corpus with the data distribution listed in Table 4. The final curated dataset spans six sources, covering both lab-controlled and in-the-wild environments, and provides diverse identities, emotional expressions, and head pose dynamics. Finally, we apply EMOCA to encode all curated videos into the FLAME parameter space, which serves for the training and evaluation of the model.

We follow a standard protocol across all datasets, reserving a small portion from each source for evaluation. As shown in Table 5, we use 11,506 videos for training and 200 videos for testing. The test set includes balanced samples from various data sources, ensuring that the evaluation addresses controlled, emotional, and in-the-wild scenarios. This split facilitates a thorough assessment of identity generalization, emotional expressivity, and head-pose dynamics under various real-world conditions.

B.2 Setup Details

The Transformer backbone of 3DXTalker is designed to balance modeling capacity and computational efficiency. It comprises 6 Transformer blocks with a hidden dimension of 768, enabling effective integration of identity, audio, and temporal cues. To better disentangle downstream targets, each prediction head (identity, pose, and expression) is equipped with two additional Transformer blocks that function as lightweight, task-specialized decoders. This hierarchical architecture ensures that shared representations capture global consistency, while branch-specific modules refine modality-dependent details.

For training, 3DXTalker is optimized for 100 epochs using 250-frame sequences and a batch size of 128, which provides a sufficient temporal window for modeling natural motions. We adopt AdamW with a learning rate of 1×10^{-4} and a weight decay of 0.01, coupled with a OneCycleLR schedule to stabilize warm-up and improve convergence. The flow-matching module operates with 512 steps during training to ensure high-fidelity trajectory learning, while 32 inference steps are used at test time to achieve a favorable balance between accuracy and generation speed.

Experiments are conducted on a shared high-performance computing cluster equipped with NVIDIA H100 GPUs. The complete training of 3DXTalker utilizes two H100 GPUs with BF16 mixed precision, resulting in a total training time of approximately five hours. Despite the shared-cluster variability, this setup demonstrates that 3DXTalker is computationally efficient and scalable for large-scale expressive talking avatar generation.

B.3 Metrics Details

We adopt 9 evaluation metrics across multiple levels, covering 3D geometry, 2D appearance, beat alignment score, and efficiency, to comprehensively assess 3D talking-avatar generation:

3D geometry.

- Lip Vertex Error (LVE) [5] measures lip synchronization by computing the mean Euclidean distance between the predicted and ground-truth lip-related mesh vertices;
- Upper Face Vertex Error (UFVE) [46] measures the mean Euclidean distance between predicted upper face mesh vertices and ground-truth;
- Upper Face Dynamics Deviation (UFDD) [44] measures the deviation in facial dynamics for motion sequences between the predicted upper face mesh vertices and the ground-truth; Both UFVE and UFDD focus on the upper face area, specifically the forehead, eye region, and nose.
- Mean Vertex Error (MVE) [15] evaluates geometric reconstruction accuracy by calculating the average Euclidean distance between corresponding vertices of the generated mesh and the ground truth across the entire head region.

2D appearance.

- Copula-based Similarity Metric (CSIM) [49] computes copula-based similarity by capturing the image features between the predicted video and ground truth per frame;
- Emotion Fréchet Distance (Emo-FID) [10] measures the similarity of emotional expressions between generated and ground-truth videos by computing the Fréchet distance between emotional embeddings extracted using the BEiT-Large model fine-tuned on AffectNet [54];
- Lip-Sync Error Confidence (LSEC) and Lip-Sync Error Distance (LSED) [55] quantify audio–2D visual sync quality through confidence and embedding-distance mismatch, as followed by SyncNet [53].

Pose alignment.

- Beat Alignment (BA) computes the average temporal distance between each audio beat and its closest motion beat.

User study.

- Mean Rank (MR) is calculated by averaging the rankings obtained from a subjective user study. As shown in Figure 9, we designed an interactive interface where participants were presented with a ground-truth identity and eight anonymized, shuffled videos generated by the comparative models. Evaluators are instructed to watch all videos and rank them from 1 (Best) to 8 (Worst) based on three criteria: identity consistency, lip synchronization, and emotional expression.

C Baseline Visualizations

We compare the performance of our 3DXTalker with seven representative baselines, as illustrated in Figure 17.

- **FaceFormer** [5]: employs an autoregressive transformer to predict 3D facial animation from speech, modeling temporal dependencies through sequential tokens.
- **CodeTalker** [44]: employs a discrete codebook representation to produce facial motions, enabling controllable audio–driven animation with compact latent tokens.
- **SelfTalk** [40]: employs a self-supervised commutative training scheme to learn 3D talking-face dynamics without paired data, enabling coherent audio–visual alignment through cycle-style consistency constraints.
- **FaceDiffuser** [46]: applies diffusion modeling in a latent motion space to generate temporally coherent 3D facial animations conditioned on speech features.

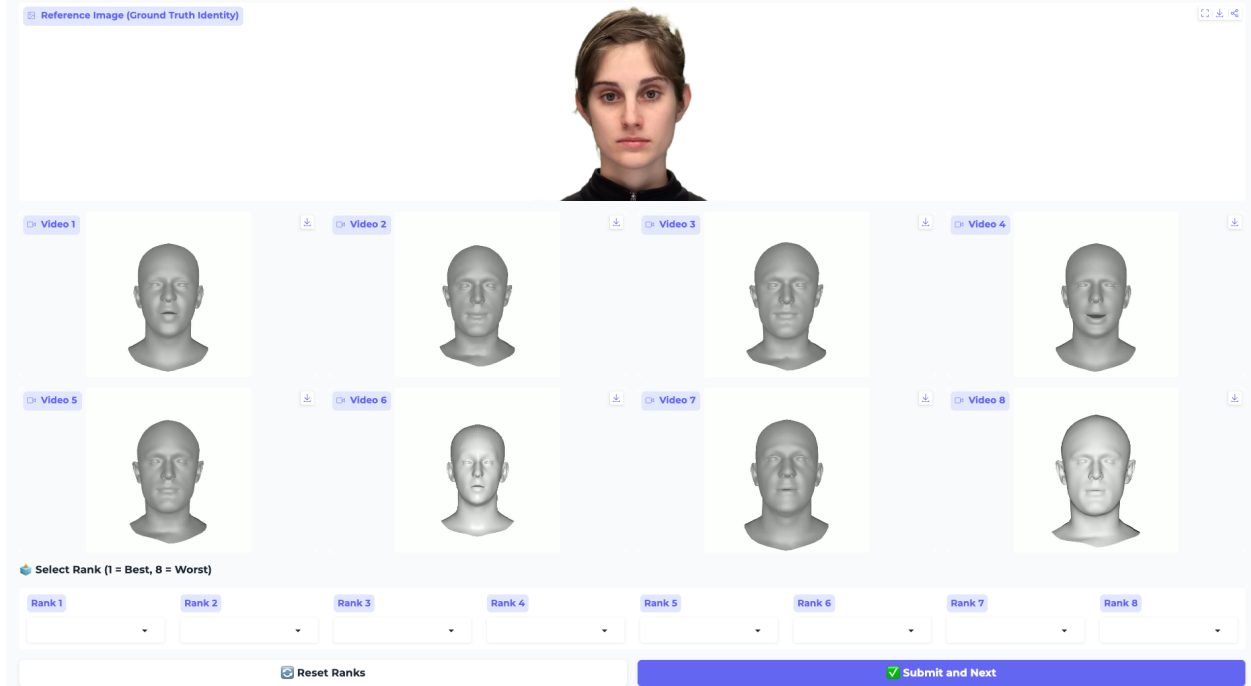


Figure 9: User study interface. Participants are presented with a ground-truth reference image (top) and eight anonymized video samples generated by all models. The videos are randomly shuffled to ensure a blind assessment.

- **EMOTE [8]**: disentangles speech content and emotion in a dual-branch architecture to drive 3D facial animation, enabling expressive emotion-aware motion generation from audio.
- **DEEPTalk [10]**: predicts FLAME expression and jaw pose in a parametric subspace using audio-aligned diffusion, focusing on emotional expressiveness and articulation accuracy.
- **DiffPoseTalk [11]**: utilizes diffusion-based regression to estimate FLAME expression and 3D head pose from audio, generating articulated facial motions with controllable pose trajectories.

D Amplitude Analysis

To further demonstrate the contribution of frame-wise amplitude embeddings, we provide more visualizations across three emotional conditions (happy, sad, and angry) as shown in Figure 10. For each example, we align the audio amplitude envelope with the corresponding phonetic segments and compare the mouth aperture generated by our full model against the variant without amplitude embeddings (w/o \mathbf{A}_{amp}). Across all emotions, our model produces mouth apertures that accurately reflect the local amplitude variations, resulting in natural changes in articulation strength. High-amplitude regions (e.g., stressed vowels and plosive consonants) correspond to visibly larger mouth apertures, while low-amplitude regions lead to more subtle movements. This demonstrates that the amplitude embedding effectively injects information about speech energy, enabling fine-grained control over lip dynamics. In contrast, the w/o \mathbf{A}_{amp} variant shows flattened or inconsistent articulation, where mouth openings vary weakly across phonemes and fail to reflect emphasis or prosodic changes. This effect is consistent across happy, sad, and angry expressions, indicating that amplitude cues are essential regardless of emotional state. Overall, these analyses confirm that amplitude embeddings enhance speech–mouth aperture alignment in 3D talking-head generation.

E Emotion Expression

E.1 Emotion Expression Template

To enable explicit global emotion control in addition to audio-driven fine-grained dynamics, we derive emotion templates directly from the FLAME expression parameter subspace. These templates represent canonical expression directions for seven basic emotions and are used for emotion scaling and interpolation during inference. MEAD dataset provides videos recorded under controlled lighting and contains high-intensity emotion performances, making it suitable for learning expression prototypes. Inspired by this, we obtain expression templates by analyzing the FLAME expression parameters ($\psi \in \mathbb{R}^{50}$) extracted by EMOCA from the MEAD dataset, with the full procedure detailed in Table 6.

Table 6: Procedure for extracting emotion templates from the MEAD dataset.

Algorithm: Extraction of Emotion Expression Templates from MEAD

Input: MEAD expression-code sessions $\{\Psi_s\}$; emotion label e .

Output: Mean template $\bar{\psi}^e$.

1. Initialize frame set: $\mathcal{X}_e \leftarrow \emptyset$.

2. For each session s containing emotion e :

Load expression sequence $\Psi_s \in \mathbb{R}^{T_s \times 50}$.

Reshape to frame-level samples.

Update frame set: $\mathcal{X}_e \leftarrow \mathcal{X}_e \cup \{\Psi_s\}$.

3. Concatenate samples across all sessions:

$$\mathcal{X}_e \in \mathbb{R}^{N_e \times 50}.$$

4. Compute mean-based template:

$$\bar{\psi}^e = \frac{1}{N_e} \sum_{i=1}^{N_e} \mathcal{X}_e[i].$$

5. Return: $\{\bar{\psi}^e\}_{e=1}^7$.

The extracted expression templates cover seven typical emotions (Angry, Contempt, Disgust, Fear, Happy, Sad, and Surprise). We further introduce a global scaling factor $\alpha \in \{1.0, 1.2, 1.4, 1.6, 1.8, 2.0\}$ to control emotion intensity, visualized in Figure 12. Naturally, some emotions (e.g., angry–disgust and surprise–fear) share similar facial muscle activation patterns, which explains the observed partial overlaps in the t-SNE space, whereas the remaining emotions form well-separated clusters (present in Figure 11). During inference, we can adjust the global emotional tone by interpolating between the reference expression ψ_{ref} and the scaled emotion template:

$$\hat{\psi}_{ref}^e = (1 - \lambda) \psi_{ref} + \lambda \alpha_e \bar{\psi}^e. \quad (11)$$

This yields seven categories of global emotion control, each with six adjustable intensities while preserving audio-driven local expression dynamics.

E.2 More Emotion Comparisons

To further demonstrate our model’s emotion expressivity, we present additional qualitative comparisons across four representative emotion categories, as shown in Figure 13. Across all categories, our model produces more expressive and coherent facial deformations, demonstrating improved emotion disentanglement and modulation compared with DEEPTalk [10] and EMOTE [8].

F Head Pose Dynamics

Expressive 3D talking avatars require coherent and flexible head pose motion in addition to accurate lip-sync and emotion-rich expressions. To better understand the controllability and behavior of the pose in the FLAME representation space, we linearly vary the θ to visualize how individual dimensions influence head motion, as illustrated in Figure 14. These variations confirm that each pose dimension corresponds to a meaningful and interpretable control component, such as pitch, yaw, roll, opening mouth, and pouting mouth, in a disentangled manner. Inspired by these disentangled pose behaviors, our 3DXTalker offers two complementary head-pose motion modes for diverse visual dynamics. First, the base model learns natural and realistic head sways directly from large-scale, in-the-wild datasets, producing subtle and coherent motions that align with the rhythm of speech. Second, 3DXTalker implements the center motion trajectory to control the head pose, along with the given direction and the deviation predicted by the model, enables diverse motion patterns, such as energetic nods, stage-presentation style, or calm, minimal movements. Figure 15 further shows the comparison of 3DXTalker with these two modes. The comparison demonstrates that the default mode emphasizes natural and subtle realism, while the trajectory-controlled mode provides significantly more diverse and controllable motion styles.

G Downstream Application

We employ ComfyUI to achieve texture mapping on the talking avatars generated by our model, using the Wan 2.2 diffusion model [56]. Wan is a versatile video generation framework that supports text-to-video, image-to-video,

and video-to-video synthesis. To align with 3DXTalker’s needs, we adopt two variants, Wan2.2-Fun-Control and Wan2.2-Speech-to-Video (S2V). Fun-Control enables fine-grained video control through depth, pose, and edge guidance, complemented by LLM-generated prompts. Specifically, we render a depth video from our 3D mesh sequence and feed it into Fun-Control to drive head pose, lip movement, and emotion-consistent facial dynamics. Meanwhile, the reference image provides identity-appearance cues, ensuring that the synthesized video maintains the subject’s visual characteristics, while the input audio provides synchronized speech. In contrast, S2V is an audio-driven video generation model that conditions on text prompts, reference images, and speech signals. It specializes in transforming a static portrait and audio into a synchronized talking video. However, unlike Fun-Control, S2V does not utilize depth guidance, which makes it less reliable in producing accurate head-pose dynamics and temporally coherent motion.

Figure 16 presents the rendered results produced using the Wan model. For each video, Wan requires two types of prompts: a positive prompt, which directs the model toward desired visual and motion characteristics, and a negative prompt, which constrains unwanted artifacts or behaviors during generation. In our setup, we vary only the positive prompts to tailor each video to its intended scene or stylistic effect while keeping the default negative prompt unchanged. This setup follows Wan’s recommended usage and ensures consistent, stable video generation across different rendering configurations. The positive prompts used for Wan rendering in Figure 16 are provided below:

- A realistic young Asian man is singing. His hair is styled in two rounded buns with red ribbons. He wears a red hoodie. He looks directly at the camera with a subtle emotional expression. Warm, fire-lit background.
- A realistic young African girl angrily speaking, with a tense brow, narrowed eyes, and tightly pressed lips. She has short natural curly hair and wears a green shirt. Strong front-facing expression, intense eye contact. Beach background with ocean and sky. Natural blinking and looking at the camera.

As shown in Figure 16, both Fun Control and S2V effectively preserve the identity and background of the reference image. Fun Control transfers identity cues to a depth-conditioned mesh. However, the reliance on a constructed depth video imposes geometric constraints, resulting in an identity that is similar to the reference. Nevertheless, it provides stable identity across the sequence and accurately follows depth-guided head motion, lip movements, and emotional cues, resulting in natural dynamics, precise lip synchronization, and coherent temporal behavior. In contrast, S2V achieves closer identity fidelity due to its 2D appearance-based generation. However, its lack of geometric grounding results in poor audio–lip synchronization and minimal head-pose variation, producing rigid and temporally inconsistent outputs. Overall, the depth-conditioned Fun Control pipeline provides stronger geometric and temporal consistency, enabling high-fidelity head motion and lip articulation that purely 2D methods cannot achieve.

In the future, to further narrow the realism gap between 3D avatars and state-of-the-art 2D talking-head models, a promising direction is to incorporate a neural rendering module on top of the predicted FLAME geometry. By learning view-dependent appearance, fine-grained facial details, and realistic skin reflectance, such a neural renderer can transform mesh outputs into photorealistic renderings while preserving the controllability of our parametric model. This hybrid geometry–appearance approach has the potential to deliver high-fidelity visual quality comparable to 2D methods without sacrificing explicit 3D structure or editing flexibility.

Instruction: You are designing a global head-pose trajectory for a 3D talking avatar. The output must correspond to the FLAME global pose parameters ($\theta^g \in \mathbb{R}^{T \times 3}$), represented as Rodrigues axis-angle vectors.

INPUTS:

- **audio:** a raw 1D NumPy array of the speech waveform (16 kHz).
- **style:** a text description of the desired singing or presentation style. (e.g., “rhythmic and energetic”, “calm and steady”, “stage-presentation style”, “passionate speech”).

Your task: Produce a Python function `head_pose_func(T, audio)` that returns a NumPy array of shape $[T, 3]$, where T is total number of frames, and each row is a Rodrigues axis angle rotation vector [pitch(y-axis), yaw(z-axis), roll(x-axis)] for the corresponding frame.

Requirements:

- Directly analyze the audio waveform to detect:
 - energy peaks (emphasis).
 - low-energy regions (pauses).
 - rhythm / periodicity cues.
- Use audio cues and a style prompt to control amplitude, pacing, and expressiveness of head motion.
- Produce smooth, continuous, interpretable trajectories.
- Ensure the resulting motion stays within natural FLAME global-pose ranges.

H Prompt Design for Motion Trajectory Control of Head Pose

To enrich spatial dynamics beyond the subtle audio-driven motion produced by 3DXTalker, we introduce an LLM-driven Cinematography strategy. This module controls head-pose motion and camera movement separately by taking an audio clip and a user prompt as input, returning smooth, interpretable motion functions that can be applied to mesh-sequence rendering. The key idea is to leverage the reasoning and generative capabilities of large language models to convert high-level textual descriptions, such as “energetic presentation”, “subtle and calm”, or “cinematic orbit shot”, into executable motion trajectories. By analyzing both the acoustic rhythm and the semantic intent provided in the prompt, the module produces parameterized functions that modulate head orientation or camera position over time, enabling expressive speaking styles and professional cinematographic effects without hand-crafted animation. This design significantly expands the range of spatial behaviors achievable by 3DXTalker, offering fine-grained control and diverse visual dynamics while preserving coherence with the underlying mesh animation. The prompt templates for both head-pose and camera-motion control are provided below.

I Discussion

While 3DXTalker demonstrates strong performance in expressive audio-driven 3D talking avatar generation, several directions remain open for future improvement.

First, the quality of the generated facial motion is inherently influenced by the modeling capacity of the underlying parametric face representation. In this work, we rely on EMOCA to lift 2D video frames into the FLAME parameter space, which enables scalable identity and motion modeling. However, the expressiveness and fidelity of the final results are ultimately bounded by the representational power of EMOCA and FLAME, particularly for subtle facial details and extreme expressions. Advances in parametric face modeling or hybrid representations may further enhance the realism and expressivity of the generated avatars.

Second, although our framework focuses on audio-driven generation, human expressive behavior is not solely determined by speech signals. Additional non-audio cues, such as linguistic content, discourse structure, or higher-level communicative intent, also play an important role in shaping expressive delivery. Incorporating such complementary signals may further enrich expressive diversity and improve alignment with user intent.

Finally, while we introduce audio-rich representations that capture frame-wise amplitude and emotion cues, modeling fine-grained emotional dynamics solely from speech remains a challenging problem. Emotional expression in speech is often subtle, context-dependent, and temporally evolving, which may not be fully captured by current audio features alone. Future work could explore more advanced affect modeling or multi-scale emotion representations to better reflect the complexity of speech-driven emotions.

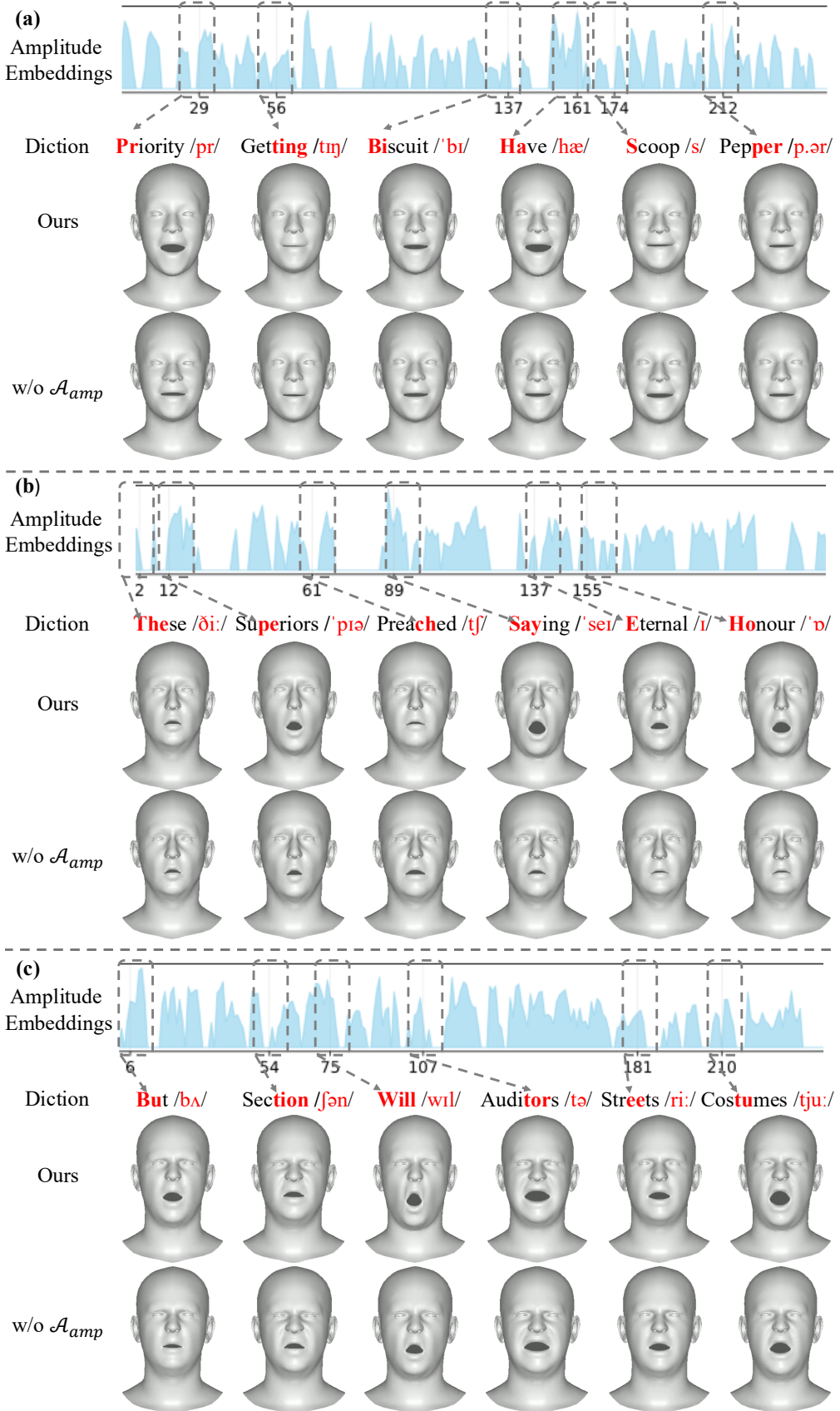


Figure 10: Amplitude analysis under different emotions, including (a) happy, (b) sad, and (c) angry.

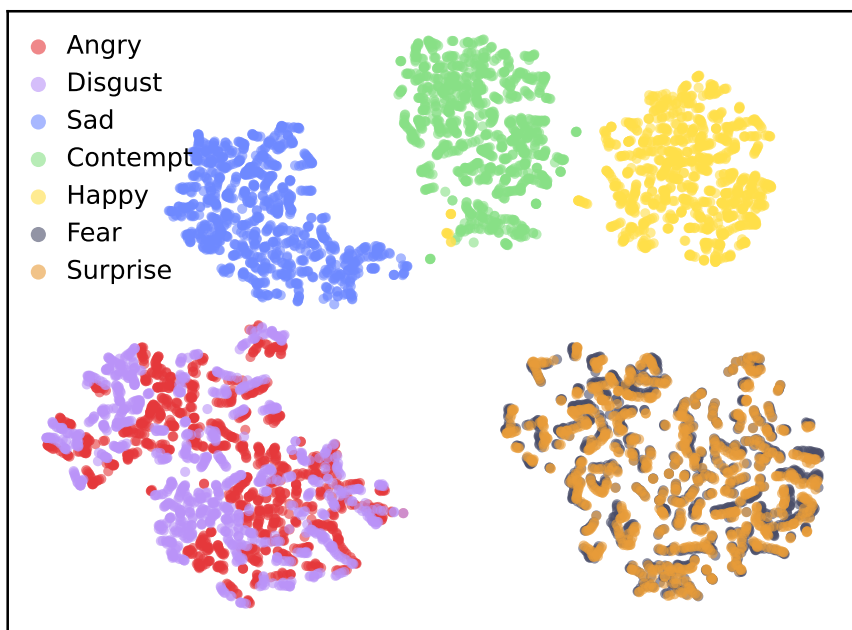


Figure 11: t-SNE visualization of our predicted expression. Partial overlaps between angry–disgust and surprise–fear correspond to their naturally similar facial activation patterns.

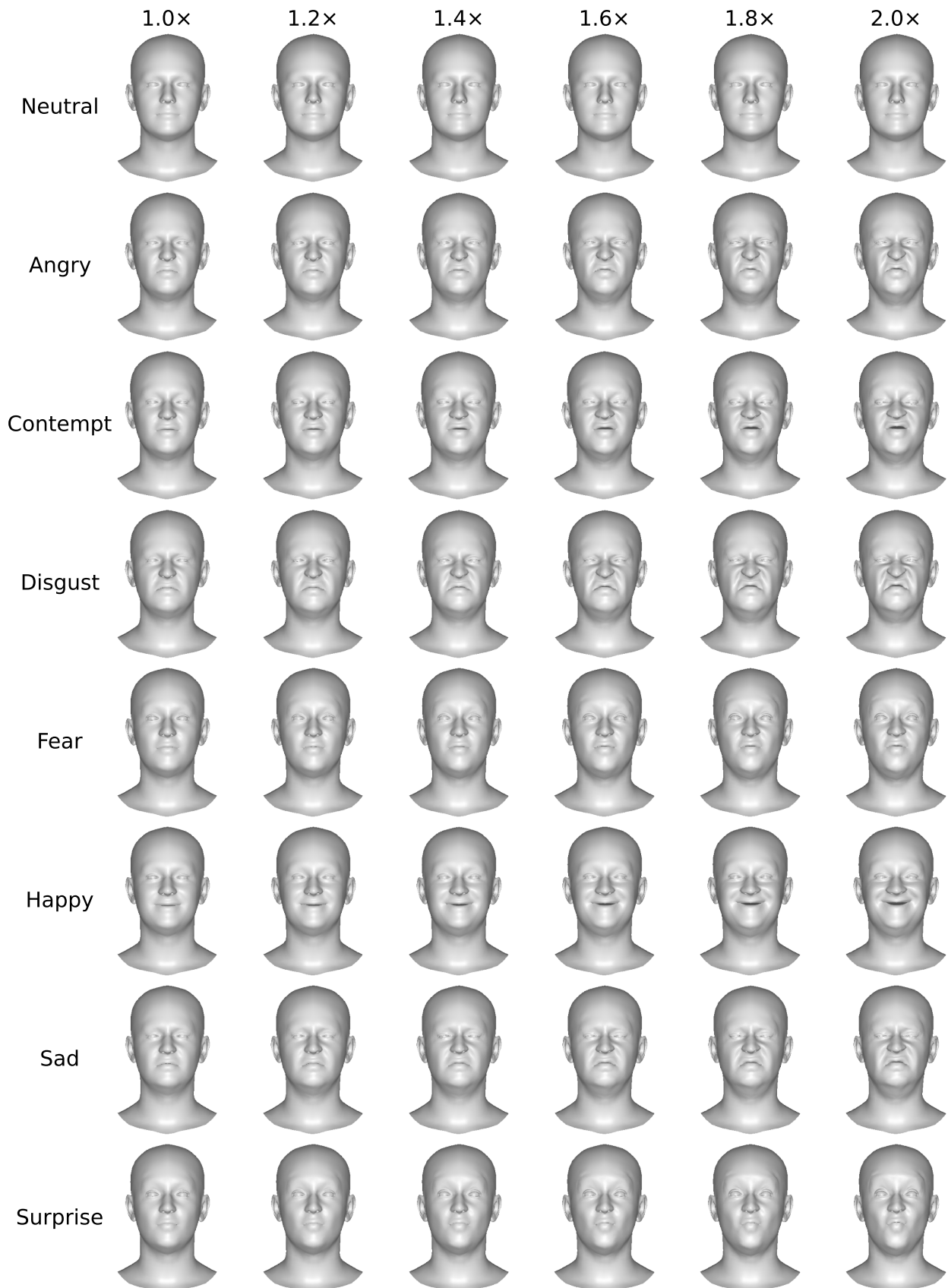


Figure 12: Neutral face (expression with zero vector) and seven emotion templates across six controllable intensity scales.

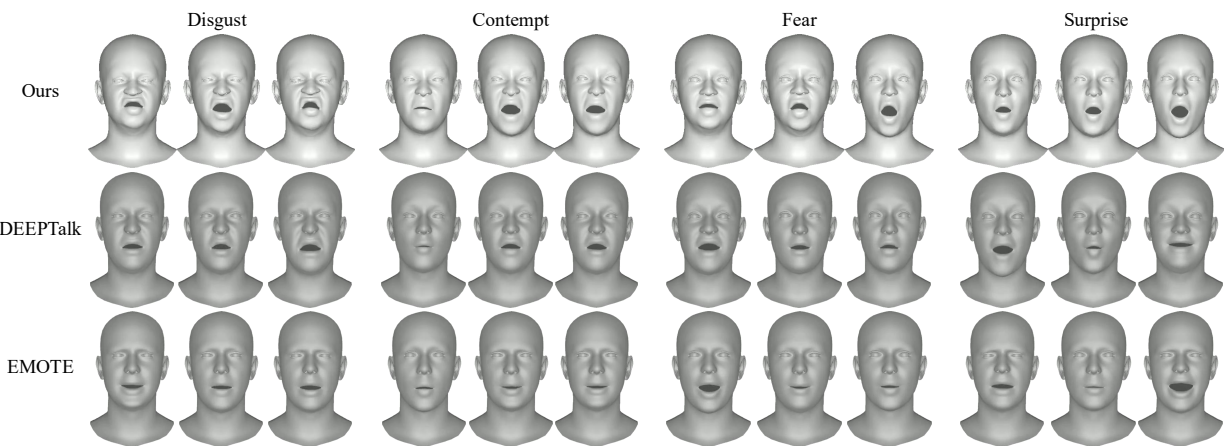


Figure 13: Additional qualitative comparisons of four emotion categories (Disgust, Contempt, Fear, Surprise) across representative baselines. 3DXTalker generates more expressive emotion patterns with clearer facial activations than DEEPTalk and EMOTE.

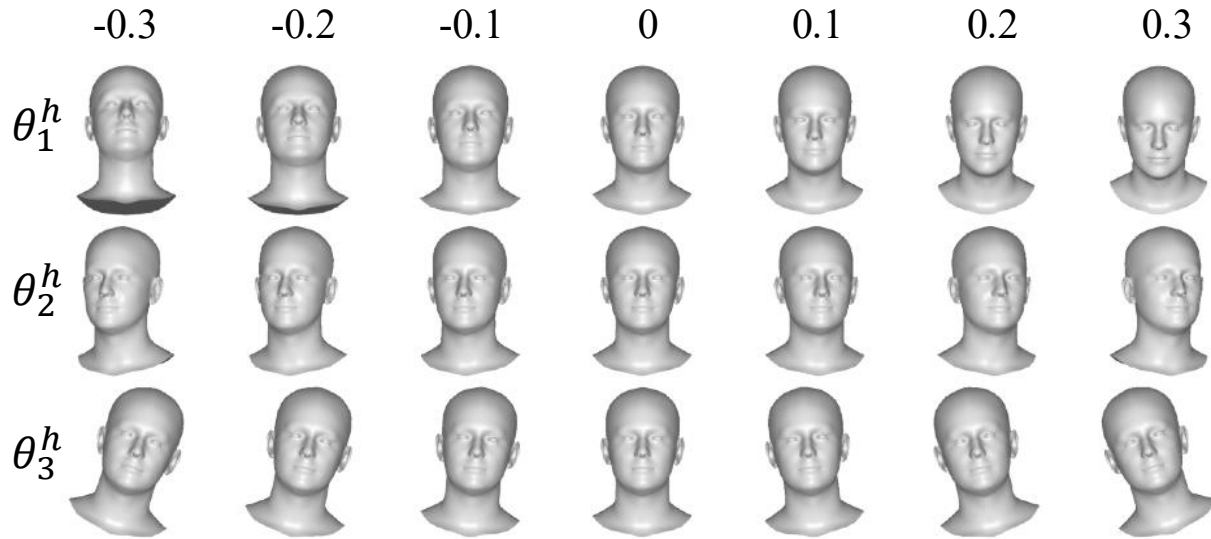
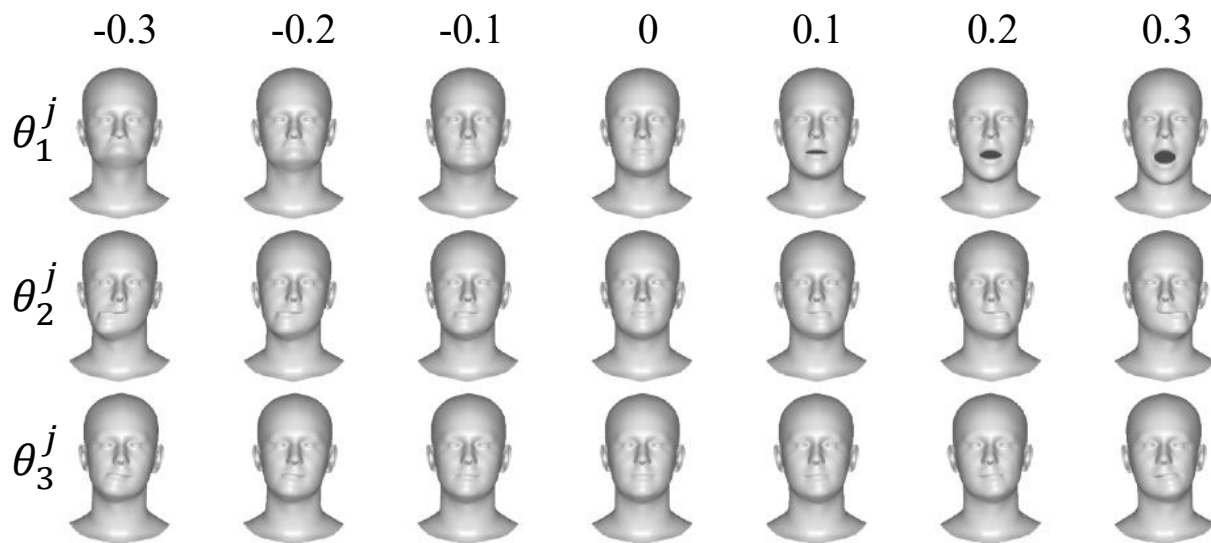
(a) Head Pose**(b) Jaw Pose**

Figure 14: Head model visualization as the control parameter θ varies. (a) three parameters for head pose; (b) three parameters for jaw pose. They vary linearly with the control parameter.

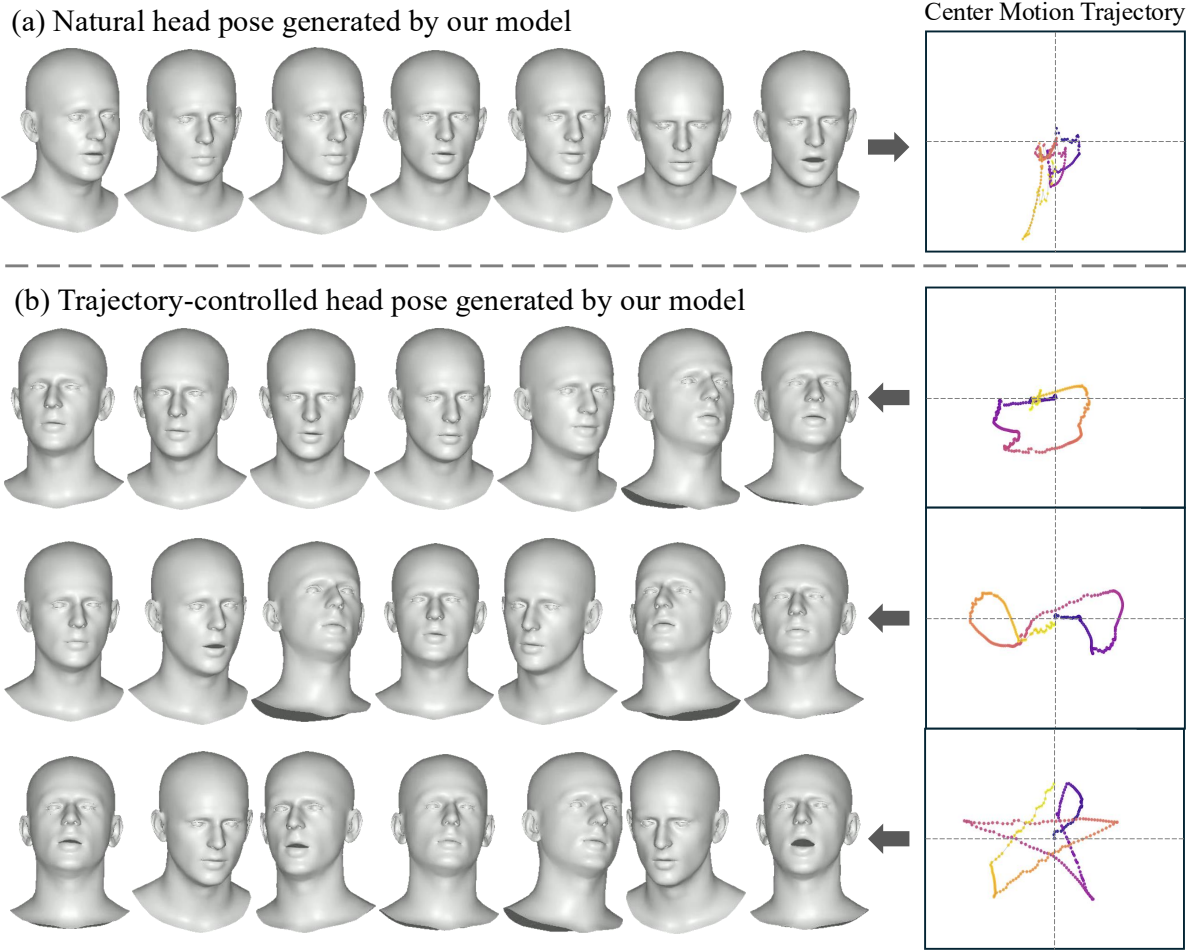


Figure 15: Comparison of head pose dynamics between the proposed natural micro-movement modeling and the trajectory-controlled head pose. By incorporating a center motion trajectory, the framework achieves both expressive flexibility and robust dynamic control. Trajectory colors indicate temporal progression (dark→light).

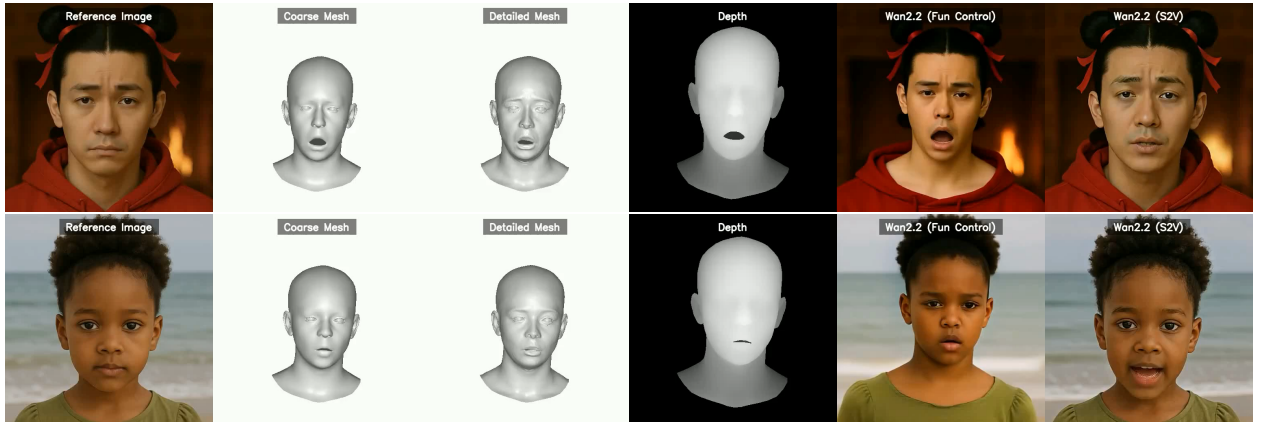


Figure 16: Wan2.2 rendering results comparison. Depth video are extracted from 3D mesh sequences generated by our 3DXTalker. Wan2.2 (Fun Control) synthesizes talking videos by conditioning on both the depth video and the reference image, while Wan2.2 (S2V) generates results directly from audio and the reference image. Both Fun Control and S2V models adopt text prompts to guide the generation process.

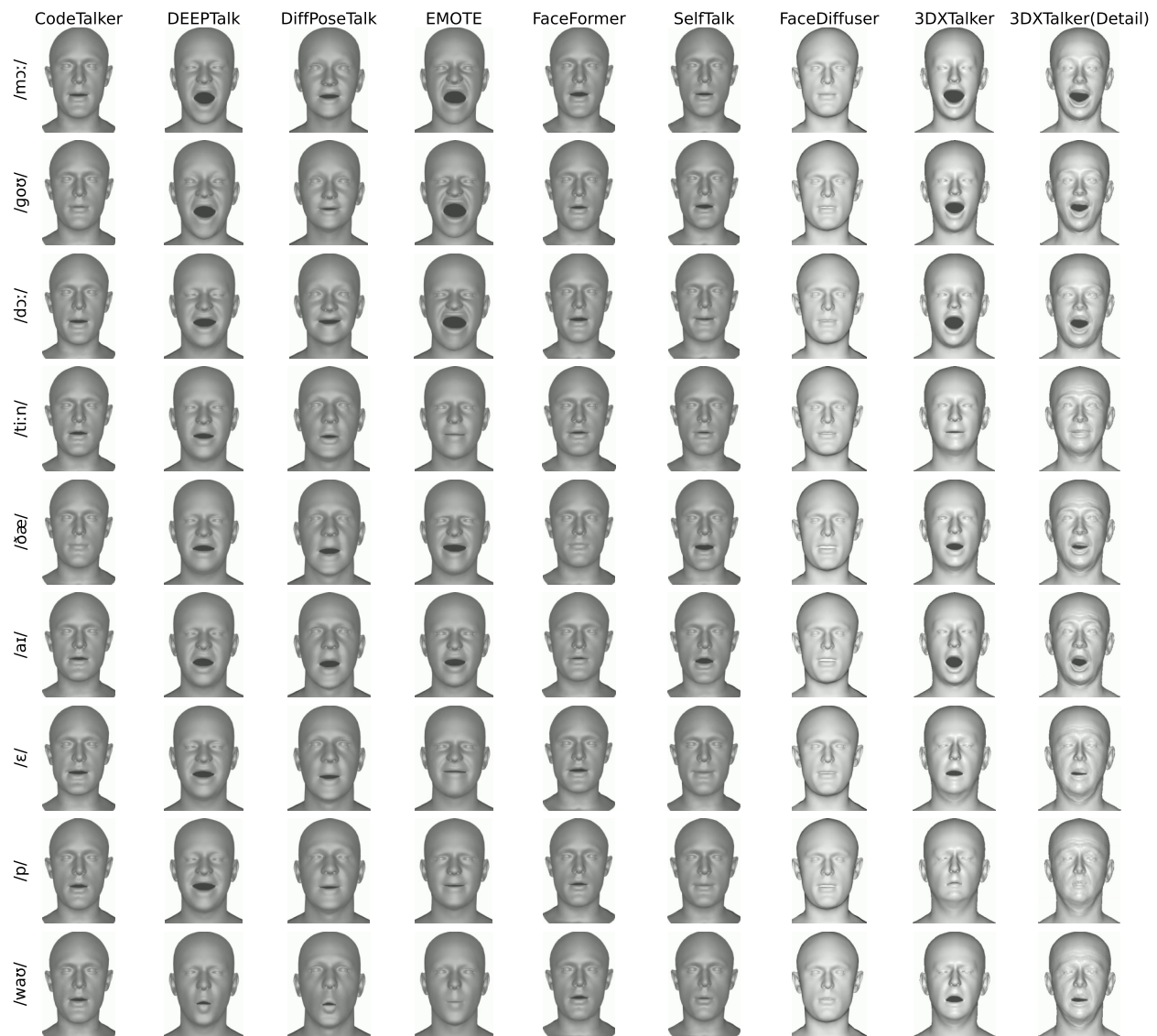


Figure 17: Visualization comparisons illustrating how mouth-aperture patterns align with phonetic symbols across different models.